



HAL
open science

Geology and radiometric dating of Quaternary monogenetic volcanism in the western Zacapu lacustrine basin (Michoacán, México): implications for archeology and future hazard evaluations

Nanci Reyes-Guzmán, Claus Siebe, Magdalena Oryaëlle Chevrel, Marie-Noëlle Guilbaud, Sergio Salinas, Paul Layer

► To cite this version:

Nanci Reyes-Guzmán, Claus Siebe, Magdalena Oryaëlle Chevrel, Marie-Noëlle Guilbaud, Sergio Salinas, et al.. Geology and radiometric dating of Quaternary monogenetic volcanism in the western Zacapu lacustrine basin (Michoacán, México): implications for archeology and future hazard evaluations. *Bulletin of Volcanology*, 2018, 80 (2), 10.1007/s00445-018-1193-5 . hal-02401449v1

HAL Id: hal-02401449

<https://uca.hal.science/hal-02401449v1>

Submitted on 14 Nov 2022 (v1), last revised 7 Mar 2023 (v2)

HAL is a multi-disciplinary open access archive for the deposit and dissemination of scientific research documents, whether they are published or not. The documents may come from teaching and research institutions in France or abroad, or from public or private research centers.

L'archive ouverte pluridisciplinaire **HAL**, est destinée au dépôt et à la diffusion de documents scientifiques de niveau recherche, publiés ou non, émanant des établissements d'enseignement et de recherche français ou étrangers, des laboratoires publics ou privés.



Distributed under a Creative Commons Attribution 4.0 International License

Geology and radiometric dating of Quaternary monogenetic volcanism in the western Zacapu lacustrine basin (Michoacán, México): implications for archeology and future hazard evaluations

Nanci Reyes-Guzmán¹  · Claus Siebe¹ · Magdalena Oryaëlle Chevrel² · Marie-Noëlle Guilbaud¹ · Sergio Salinas³ · Paul Layer⁴

Abstract

The Zacapu lacustrine basin is located in the north-central part of the Michoacán-Guanajuato volcanic field (MGVF), which constitutes the west-central segment of the Trans-Mexican Volcanic Belt. Geological mapping of a 395 km² quadrangle encompassing the western margin of the basin, ⁴⁰Ar/³⁹Ar and ¹⁴C radiometric dating, whole-rock chemical and petrographic analyses of volcanic products provide information on the stratigraphy, erupted volumes, age, and composition of the volcanoes. Although volcanism in the MGVF initiated since at least 5 Ma ago, rocks in the western Zacapu lacustrine basin are all younger than ~2.1 Ma. A total of 47 volcanoes were identified and include 19 viscous lava flows (~40 vol.%), 17 scoria cones with associated lava flows (~36 vol.%), seven lava shields (~15 vol.%), three domes (~6 vol.%), and one maar (~2 vol.%). Erupted products are dominantly andesites with 42 km³ (~86 vol.%) followed by 4 km³ of dacite (~8 vol.%), 1.4 km³ of basaltic trachy-andesite (~3 vol.%), 1 km³ of basaltic andesite (~2 vol.%), and 0.14 km³ of rhyolite (~0.3 vol.%). Eruptive centers are commonly aligned ENE-WSW following the direction of the regional Cuitzeo Fault System. Over time, the high frequency of eruptions and consequent accumulation of lavas and pyroclastic materials pushed the lake's shore stepwise toward the southeast. Eruptions appear to have clustered through time. One cluster occurred during the Late Pleistocene between ~27,000 and ~21,300 BC when four volcanoes erupted. A second cluster formed during the Late Holocene, between ~1500 BC and ~AD 900, when four closely spaced monogenetic vents erupted forming thick viscous 'a'a to blocky flows on the margin of the lacustrine flats. For still poorly understood reasons, these apparently inhospitable lava flows were attractive to human settlement and eventually became one of the most densely populated heartlands of the pre-Hispanic Tarascan civilization. With an average eruption recurrence interval of ~900 years during the Late Holocene the western Zacapu lacustrine basin is one of the most active areas in the MGVF and should hence be of focal interest for regional volcanic risk evaluations.

Keywords Zacapu basin · Michoacán-Guanajuato volcanic field · Quaternary · Monogenetic cluster · Radiocarbon · ⁴⁰Ar/³⁹Ar dating · *Malpais*

Editorial responsibility: R.J. Brown

✉ Nanci Reyes-Guzmán
nanreyguz@gmail.com

¹ Departamento de Vulcanología, Instituto de Geofísica, Universidad Nacional Autónoma de México, C.P. 04510 Coyoacán, Mexico

² Université Clermont Auvergne, CNRS, IRD, OPGC, Laboratoire Magmas et Volcans, F-63000 Clermont-Ferrand, France

³ División de Ingeniería en Ciencias de la Tierra, Facultad de Ingeniería, Universidad Nacional Autónoma de México, C.P. 04510 Coyoacán, Mexico

⁴ Department of Geology and Geophysics, University of Alaska Fairbanks, Fairbanks, AK, USA

Introduction

The Trans-Mexican Volcanic Belt (TMVB) is an active volcanic arc related to the subduction of the Cocos Plate underneath the North America Plate along the Middle America trench (e.g., Demant 1978; see inset map in Fig. 1). This arc forms an angle of ~15° with respect to the trench and traverses the Mexican Altiplano, a highland characterized by active normal faulting and horst-and-graben structures that resulted in the formation of basins often occupied by broad (but shallow) lakes such as the Pátzcuaro, Cuitzeo, and Zacapu lakes in Michoacán (Johnson and Harrison 1990, see also Fig. 1). These lakes have been of interest for their archeological

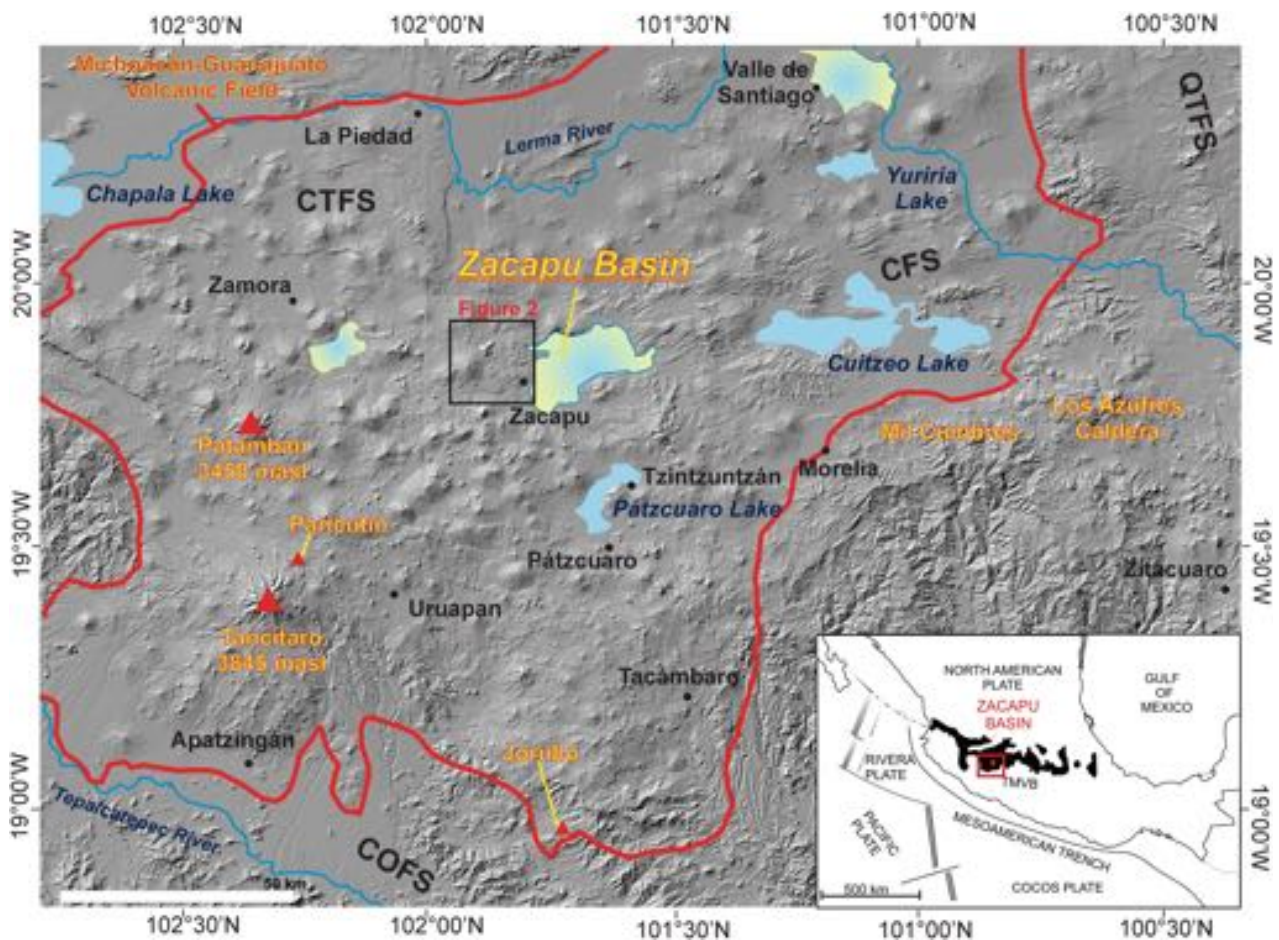


Fig. 1 Digital elevation model of the Michoacán-Guanajuato volcanic field (MGVF) showing the location of the Zacapu basin and the study area (black rectangle denotes area covered in Fig. 2). Major fault systems are: CFS=Cuitzeo Fault System, CTFS=Chapala-Tula Fault System,

COFS=Chapala-Oaxaca Fault System, QFTS = Querétaro-Taxco Fault System. Inset map at lower right corner shows location of the MGVF within the TMVB (modified after Kshirsagar et al. 2015)

records because the favorable aquatic and riparian conditions attracted early nomadic humans and promoted the development of agriculture in the Michoacán region and eventually became a major dwelling hub for the pre-Hispanic populations. The Tarascans, also known as *Purépechas*, founded one of the largest empires of Mesoamerica during the Middle/Late Postclassic period (AD 1250–1521) around lake Pátzcuaro; however, their predecessors resided mainly near riverine valleys and lakes including the area of the Zacapu basin (Pollard 1993; O’Hara et al. 1993).

The TMVB is formed of ~ 8000 volcanic vents that include calderas, stratovolcanoes, medium-sized shield volcanoes, scoria cones with associated lava fields, lava domes, and maars volcanoes. The highest concentration of monogenetic vents is found in the Michoacán-Guanajuato volcanic field (MGVF; Hasenaka and Carmichael 1985b) located in the west-central part of the TMVB. In this paper, we focus on a small, but geologically very active area at the western margin of the Zacapu lacustrine basin located in the north-central part

of the MGVF (Fig. 1). This area experienced several eruptions during the Late Pleistocene-Holocene and includes the present medium-sized city of Zacapu, as well as several important archeological sites (e.g., Pereira et al. 2017, in press). Therefore, in the present study, it is not only of volcanological interest (e.g., for hazard evaluations) but also of relevance for understanding the prehistory of Michoacán.

Geological setting

The Michoacán-Guanajuato volcanic field

The MGVF has the highest concentration of monogenetic volcanoes in the entire TMVB and occupies an area of ~ 40,000 km². It hosts > 1000 small monogenetic volcanoes, mainly scoria cones, that include the historical Jarulló (1759–1774; Guilbaud et al. 2011; Rasoazanamparany et al. 2016) and Parícutin volcanoes (1943–1952; Luhr and Simkin

1993; Pioli et al. 2008). In addition, shields, domes, viscous lava flows, and rare maars occur (Hasenaka and Carmichael 1985a, 1987; Hasenaka 1994; Guilbaud et al. 2011, 2012; Pola et al. 2014; Kshirsagar et al. 2015; Chevrel et al. 2016a, b; Mahgoub et al. 2017a). Furthermore, the MGVF encloses two stratovolcanoes: Tancitaro and Patambán, both probably extinct (Ownby et al. 2007; Siebe et al. 2014). The small-to-medium-sized volcanoes of the MGVF were classified by Hasenaka (1994) into A-type and B-type shield volcanoes, lava domes and flows, and composite volcanoes. According to this author, the shields (“Mexican shields”) are 2–12 km in basal diameter, 100–1000 m in height, and 0.5 to 10 km³ in volume. A-type and B-type shield volcanoes have gentle slope angles around 5° and 10°, respectively, while lava domes have higher slope angles (> 15°). Lava flows can be associated with a scoria cone or have hidden vents, and their average thickness is widely variable (< 100 m). In his work Hasenaka (1994) estimated that the average volcanic output rate for the last 1 Ma in the MGVF was 0.7 km³/ka, whereas the rate for the preceding period (3–1 Ma) was much less (0.2 km³/ka).

The causes for the existence of such a great number of monogenetic volcanoes in the MGVF, which is also the region where the TMVB is widest, are still poorly understood. Their high density may be related to the “peculiar” geometric configuration of the subduction zone (Pardo and Suárez 1995; Johnson et al. 2009; Blatter and Hammersley 2010) that controls the location and size of magma generation areas and the magnitude of crustal extension. As proposed by Chevrel et al. (2016b), the large number of monogenetic volcanoes in the MGVF might be related to the flat position at a depth of 90–120 km of this segment of the subducting oceanic Cocos plate underneath the continental North America Plate (Kim et al. 2012). Such a low subduction angle at depth might be inducing partial hydrous melting of the mantle wedge (Carmichael 2002) over a wide area underneath a ~40-km-thick continental crust.

The Zacapu intermontane basin

The Zacapu intermontane basin is a tectonic basin whose lowest part (1980 m asl) is today occupied by a cultivated flat surface of lacustrine origin that is surrounded by Plio-Quaternary volcanoes that are mostly intermediate (calc-alkaline basaltic andesite to andesitic) in composition (Demant 1992; Siebe et al. 2013). Fewer silicic rocks (dacites and rhyolites) also occur as domes and ignimbrite sheets (Kshirsagar et al. 2015). The area is a graben structure with normal faults and forms the western extent of the seismically active Cuitzeo Fault System (CFS in Fig. 1; Johnson and Harrison 1990), also called the Morelia-Acambay Fault System (Suter et al. 2001; Garduño-Monroy et al. 2009).

The study area (Fig. 2) is located immediately west of the lacustrine flat and to the northwest of the city of Zacapu. It is cut by active normal faults such as the Villa Jiménez fault, visible in the northeastern part of the mapped quadrangle, where it cuts the Brinco del Diablo shield forming a prominent scarp (Demant 1992). All of these faults belong to the Cuitzeo Fault System that follows a N65°E to N85°E trend (Kshirsagar et al. 2015, 2016). Since volcanic vents are frequently aligned in this direction, we presume that eruptions were fed by dikes emplaced along these faults during final magma ascent. A characteristic feature of this part of the lacustrine basin is the young age of the volcanic cover (< 2.1 Ma) and the smaller variation of its chemical composition (Siebe et al. 2013), if compared to other areas in the MGVF.

The current lacustrine Zacapu basin underwent a continuous and active paleoclimate evolution since its formation during the Late Pliocene-Pleistocene (3–1 Ma) related to the development of an extensional tectonic regime (Demant 1992; Pétrequin 1994). Shallow drillings into the lake sediments were undertaken to investigate its paleoclimatic history and Lozano-García and Xelhuantzi-López (1997) and Metcalfe (1997) reported significant variations of the lake level, which these authors related mostly to temperature and precipitation changes. However, the evolution of the lacustrine environment has also been influenced by volcanic, tectonic, as well as human activity (Ortega-Guerrero et al. 2002). The latter initiated at least ~3000 years ago, as evidenced by *Zea mays* (corn) in pollen records from lake beds in Michoacán (first detected in lake Pátzcuaro by Watts and Bradbury 1982, also reported from lake Zirahuén by Torres-Rodríguez et al. 2012).

The volcanically young area on the western shore of the Zacapu lacustrine basin is of archeological relevance to better understand the development of the Tarascan Empire. Zacapu means “stony place” in Purhépecha (the native language of the Tarascan people) and refers to the young lava flows that occur in the vicinity of Zacapu city. These flows are collectively called Malpaís de Zacapu. *Malpaís* means badlands in Spanish and is a local term for young sparsely vegetated lava flows (mainly andesites), which in this case are up to 100 m thick and have a rough blocky surface almost devoid of soil. Despite their inhospitable appearance (moon-like landscape, unsuitable for agriculture), several of these lava flows were densely inhabited in pre-Hispanic time (before AD 1521) as attested by numerous archeological remains (Migeon 1998). In the case of the Malpaís de Zacapu (a cluster of four young lava flows that issued from different vents, namely El Infiernillo, Malpaís Las Víboras, El Capaxtiro, and Malpaís Prieto, in chronological order of eruption, see also Mahgoub et al. 2017b), the human occupation from AD 1250 to 1400 was very intense (at least 10,000 inhabitants, as judged by the number of housing

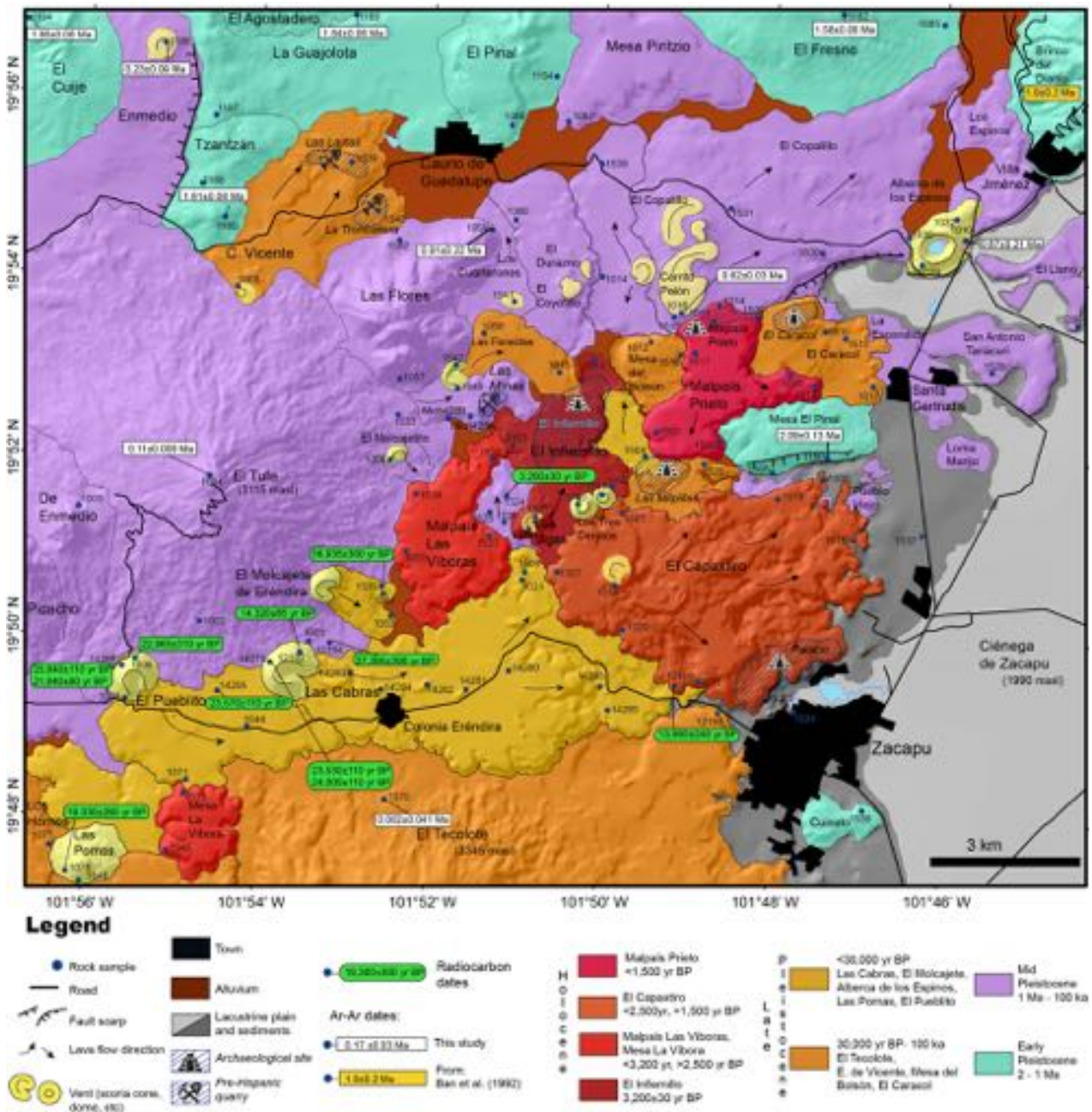


Fig. 2 Geologic map of the western part of the Zacapu lacustrine basin. Sample locations (radiometric dates, paleosols, and geochemistry) are also indicated

foundations, Michelet et al. 2005; Michelet, 2010). This paradox (dense population on apparently inhospitable substrate) has as of today not been solved satisfactorily, although several explanations have been proposed. Interestingly enough, the case of the Malpais de Zacapu is not unique, since archeological sites indicating large population centers on young lava flows at the margins of lakes have been excavated elsewhere in the Trans-Mexican Volcanic Belt and include Urichu (Pollard and Cahue 1999; Pollard 2003) and Angamuco (Fisher and

Leisz 2013; Fisher et al. 2017) in the eastern and western Pátzcuaro basin respectively, Cantona in the Serdán-Oriental basin of eastern Puebla (García-Cook 2003), and Teotenango in the southern Toluca (upper Lerma) basin (Piña-Chan 1972).

For these reasons (archeological importance and evaluation of past and future impacts on populations), we established the chronological sequence of the volcanic eruptions in this area, including their eruptive styles, volumes, and compositions.

Methods

Fieldwork

For the geological map (Fig. 2), the limits of the different volcanoes in the study area were first drawn with the aid of 1:50,000 satellite images and topographic maps from the Instituto Nacional de Estadística, Geografía e Informática (INEGI), a digital elevation model (DEM) at a 15-m horizontal resolution built using ArcView Geographic Information Systems (ArcGis), and a high-resolution light detection and ranging (LIDAR) image acquired for the MESOMOBILE archeological project directed by Grégory Pereira and Véronique Darras (CNRS/ Université Paris 1, Panthéon-Sorbonne, Paris, France).

During fieldwork, we explored all roads including unpaved dirt tracks and hiked along geologic contacts to confirm their limits, collect rock samples, and determine the stratigraphic sequence of the volcanic units. In total, we collected 122 rock and 12 paleosol samples for the purpose of petrographical and chemical analyses (major and trace elements), as well as $^{40}\text{Ar}/^{39}\text{Ar}$ dating, and radiocarbon dating, respectively.

Analytical procedures

From the 122 collected rock samples, 93 were crushed using steel-tools contaminating less than 0.1 wt.% with Fe and chemically analyzed at Activation Laboratories LTD (Ancaster, Canada) by a combination of methods that include fusion-inductively coupled plasma (FUS-ICP), total-digestion inductively coupled plasma (TD-ICP), and multi-instrumental neutron activation analysis (INAA). For further details of the analytical procedures see Agustín-Flores et al. (2011) and the Activation Laboratories website. Magma types were defined from the major element data and recalculated to 100 vol.% (anhydrous basis), following recommendations from the International Union of Geological Sciences (Le Maitre 2002). In addition, 75 polished thin sections were prepared. The analysis revealed a wide range of compositions from basaltic andesite to rhyolite ($\text{SiO}_2 = 55\text{--}76$ wt.%). The full chemical data set will be presented elsewhere.

Ten rock samples were irradiated at McMaster University in Hamilton, Ontario, Canada and the mineral TCR-2 with an age of 28.619 Ma (Renne et al. 2010) was used to monitor neutron flux and calculate the irradiation parameter. The samples were then dated by the $^{40}\text{Ar}/^{39}\text{Ar}$ method at the Geophysical Institute, University of Alaska, Fairbanks. Procedures are described in Layer (2000) and Guilbaud et al. (2011, 2012). A summary of the results is shown in Table 1, and age spectra and inverse isochron plots are shown in Fig. 3a, b for Early and Middle to Late Pleistocene volcanic rock samples, respectively.

Table 1 $^{40}\text{Ar}/^{39}\text{Ar}$ Ar dates for volcanic rocks in the western Zacapu basin area, Michoacán. All errors quoted at the 1-sigma level, the plateau age is the preferred age and was calculated using the TCR-2 standard with an age of 28.619 Ma (Renne et al. 2010). Sample type: volcanic glass and plagioclase. N: number of stages used in plateau or isochron, MSDW mean square of weighted deviates

| Volcano | Sample | Latitude (N) | Longitude (W) | Integrated age (Ma) | Isoc. # frac. | Isoc. $^{40}\text{Ar}/^{39}\text{Ar}$ | Isoc. MSDW | Isochron age (Ma) | Plat. # frac. | Plat. $\%^{39}\text{Ar}$ | Plat. MSDW | Plateau age (Ma) |
|------------------------|-----------|--------------|----------------|---------------------|---------------|---------------------------------------|------------|-------------------|---------------|--------------------------|------------|------------------|
| Early Pleistocene | | | | | | | | | | | | |
| Mesa El Pinal | ZAC-1190 | 19°52'00.5" | 101° 47' 33.5" | 2.066 ± 0.146 | 7 of 7 | 290 ± 10 | 0.12 | 2.193 ± 0.126 | 5 of 7 | 93 | 0.16 | 2.095 ± 0.127 |
| El Agostadero | ZAC-1189 | 19°57'06.2" | 101° 54' 31.3" | 1.692 ± 0.085 | 7 of 7 | 261 ± 13 | 0.09 | 1.937 ± 0.071 | 5 of 7 | 87 | 0.38 | 1.840 ± 0.057 |
| El Cuije | ZAC-1194 | 19°57'43.5" | 101° 56' 44.4" | 1.425 ± 0.204 | 7 of 7 | 284 ± 8 | 0.22 | 1.691 ± 0.065 | 4 of 7 | 77 | 0.39 | 1.664 ± 0.062 |
| Tzantán | ZAC-1185B | 19°54'31.5" | 101° 54' 23.8" | 1.681 ± 0.094 | 7 of 7 | 301 ± 9 | 0.22 | 1.572 ± 0.121 | 5 of 7 | 71 | 0.01 | 1.610 ± 0.084 |
| El Fresno | ZAC-1182 | 19°58'36.4" | 101° 48' 39.2" | 1.577 ± 0.062 | 5 of 7 | 297 ± 18 | 0.3 | 1.557 ± 0.078 | 5 of 7 | 94 | 0.38 | 1.579 ± 0.058 |
| Middle Pleistocene | | | | | | | | | | | | |
| Las Flores | ZAC-1059 | 19°54'31.5" | 101° 51' 16.6" | 0.877 ± 0.210 | 7 of 7 | 289 ± 17 | 0.09 | 1.140 ± 0.728 | 5 of 7 | 93 | 0.03 | 0.912 ± 0.219 |
| Alberca de los Espinos | ZAC-1010C | 19°54'16.4" | 101° 46' 22.0" | 0.788 ± 0.207 | 6 of 7 | 287 ± 17 | 0.21 | 1.430 ± 0.998 | 4 of 7 | 94 | 0.29 | 0.870 ± 0.213 |
| Cerrito Pelón | ZAC-1016 | 19°53'33.1" | 101° 49' 01.4" | 0.559 ± 0.041 | 9 of 9 | 271 ± 7 | 0.14 | 0.691 ± 0.035 | 4 of 9 | 92 | 0.82 | 0.620 ± 0.033 |
| Enmedio | ZAC-1188 | 19°56'24.0" | 101° 55' 04.1" | 0.242 ± 0.093 | 7 of 7 | 303 ± 21 | 0.19 | 0.151 ± 0.227 | 5 of 7 | 93 | 0.21 | 0.229 ± 0.093 |
| El Tule | ZAC-1004 | 19°51'41.0" | 101° 54' 31.2" | 0.128 ± 0.009 | 9 of 11 | 309 ± 18 | 0.24 | 0.096 ± 0.026 | 6 of 11 | 85 | 0.42 | 0.116 ± 0.008 |
| El Tecolote | ZAC-1070 | 19°48'09.9" | 101° 52' 26.7" | - 0.018 ± 0.045 | 7 of 7 | 283 ± 16 | 0.12 | 0.042 ± 0.058 | 5 of 7 | 96 | 0.08 | 0.002 ± 0.041 |

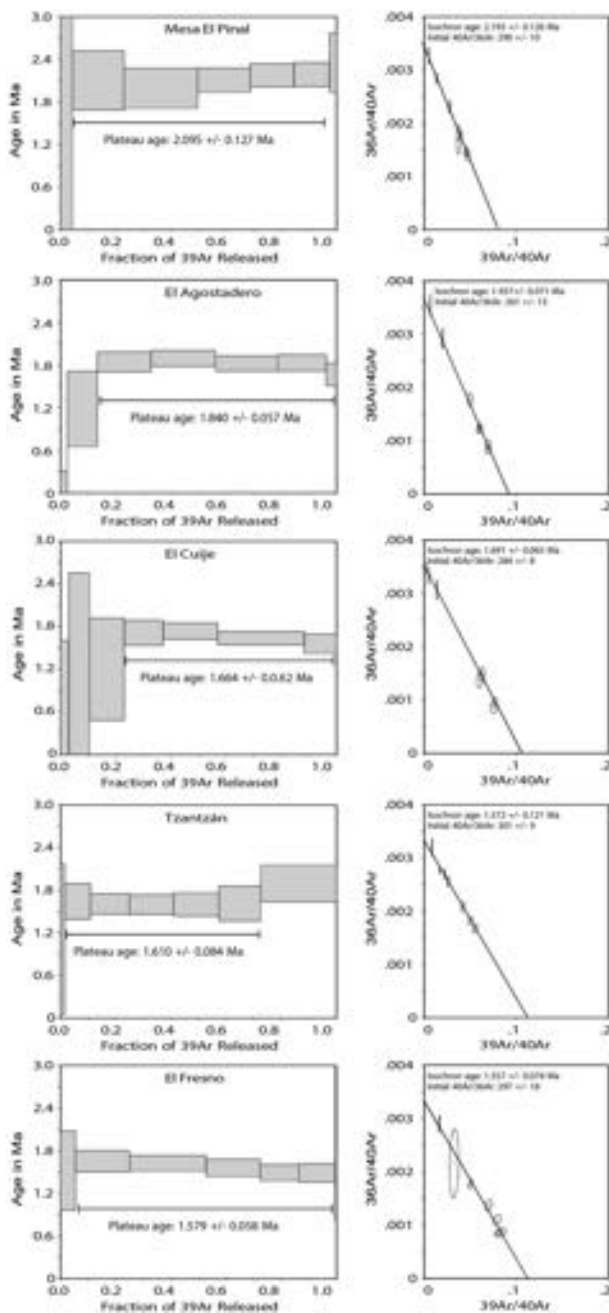


Fig. 3 **a** $^{40}\text{Ar}/^{39}\text{Ar}$ age spectra and inverse isochron plots of Early Pleistocene volcanic rock samples. **b** $^{40}\text{Ar}/^{39}\text{Ar}$ age spectra and inverse isochron plots of Middle and Late Pleistocene volcanic rock samples

Additionally, 12 paleosol samples were collected for radiocarbon dating (Table 2). Most stem from the first 2 cm underlying directly ash fallout deposits (Fig. 4) and were dated either by the conventional radiocarbon (^{14}C) method at the Department of Geosciences, University of Arizona, Tucson or by the accelerator mass spectrometry (AMS) method at Beta Analytic Inc., Miami, FL. The dates obtained were calibrated to calendar years by applying the Stuiver and Reimer

(1993) procedure and with the help of the CALIB computer program (version 7.1, IntCal13 calibration curve).

Stratigraphy ($^{40}\text{Ar}/^{39}\text{Ar}$ and ^{14}C ages)

Plio-Quaternary volcanoes up to 5 Ma in age (Siebe et al. 2014) surround the Zacapu lacustrine basin, which is filled by sediments of unknown thickness derived from them. The nature of the regional basement is also uncertain due to the extensive young volcanic cover, although xenoliths of lavas and ignimbrites have been reported from the Alberca de Guadalupe maar deposits (Kshirsagar et al. 2015) in the SE part of the basin. The oldest dated rocks in the region (4.526 ± 0.016 Ma) crop out at Cerro La Sanabria (Kshirsagar et al. 2015), located at the NE limit of the basin, well outside of the present study area.

The oldest volcanoes within the study area are Early Pleistocene (2–1 Ma) in age (Fig. 2), and several of them were dated by the $^{40}\text{Ar}/^{39}\text{Ar}$ method (Table 1, Fig. 3a). The oldest dated rock is Mesa El Pinal lava flow (Fig. 5a, b, d) with 2.095 ± 0.13 Ma; however, La Guajolota lavas (NW limit of the study area) might be older based on their geomorphology. Moreover, the southern lava front of El Agostadero shield dated at 1.84 ± 0.06 Ma leans against La Guajolota lava flow. In other words, La Guajolota was probably erupted first, followed in chronological order by Mesa El Pinal, Brinco del Diablo shield (NE corner of the study area, dated by Ban et al. 1992 by the K-Ar method at 1.9 ± 0.2 Ma), Cuinato and El Pinal lava flows (none of them dated, but morphologically comparable), El Agostadero (1.84 ± 0.06 Ma), El Cuije shield (1.66 ± 0.06 Ma), Tzatzán lava flow (1.61 ± 0.08 Ma), and finally El Fresno shield (1.58 ± 0.06 Ma). A distinct feature of these Early Pleistocene volcanoes is that they are all visibly affected by normal faulting, as evidenced by linear cliff-forming escarpments (see Fig. 5d showing Mesa El Pinal dissected by a prominent ENE-WSW trending fault belonging to the Cuitzeo Fault System).

Based on few $^{40}\text{Ar}/^{39}\text{Ar}$ dates (Fig. 3b) combined with stratigraphic relations and morphological features (e.g., depth of erosion channels, soil thickness, etc.), we established a chronological sequence of the eruptions that occurred in the Mid-Pleistocene (1 Ma–100 ka). Los Cuarterones lava flow was erupted before the emplacement of Las Flores dome complex (Fig. 5c) dated at 0.92 ± 0.22 Ma and Las Minas lava flow. Then, lava flows and scoria cones near the NW margin of the basin including Los Espinos lava flow (0.87 ± 0.21 Ma), El Copalillo-Cerrito Pelón (0.62 ± 0.03 Ma), Enmedio cone (0.23 ± 0.09 Ma), El Molcayetito, El Coyotillo-El Durazno, and contemporaneous Mesa Pirtizio lava flows were emplaced, followed by the much more voluminous Picacho, De Enmedio, and El Tule (Fig. 5a, b, e) shields, the latter dated at 0.11 ± 0.008 Ma.

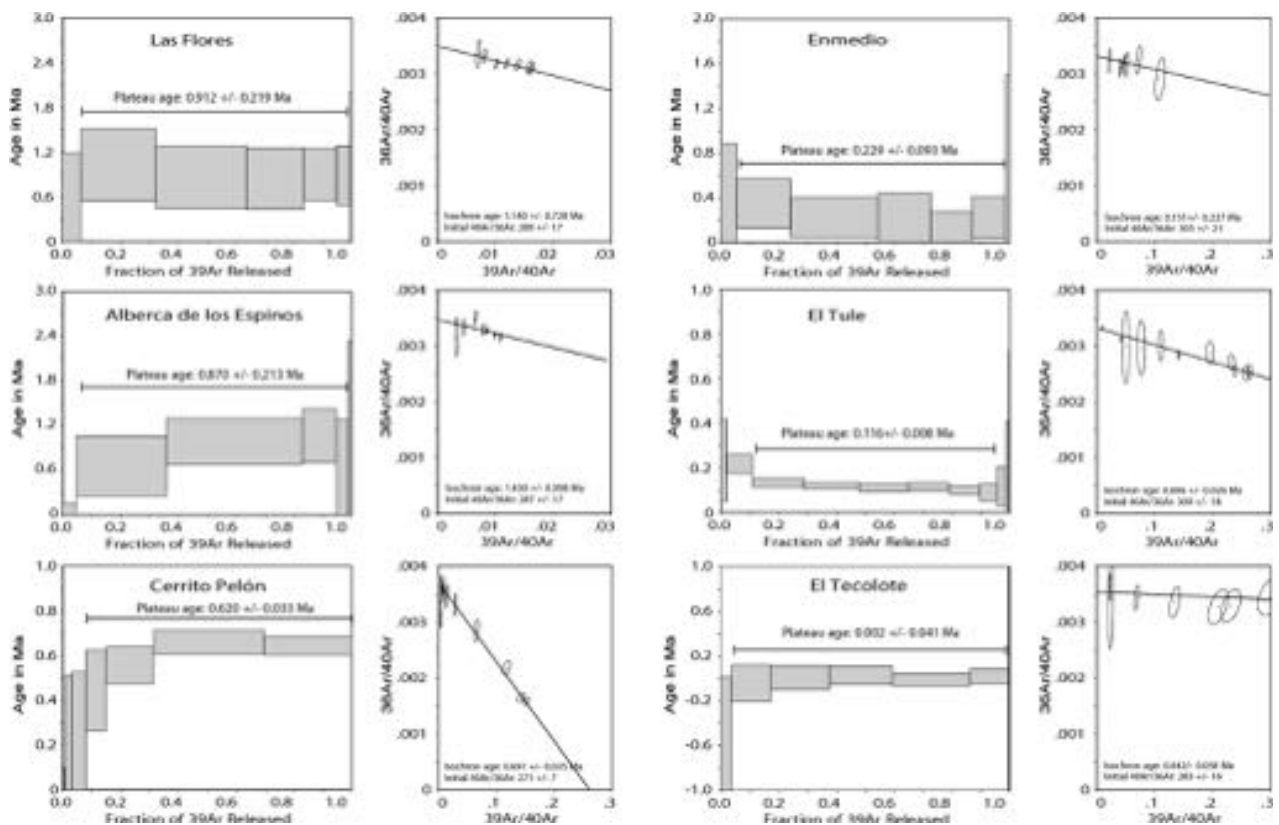


Fig. 3 continued.

For the Late Pleistocene (100–11 ka), stratigraphic relations and morphological observations were combined with radiometric dates obtained by the ^{14}C - method (Table 2 and Fig. 4) to establish a chronological sequence. ^{14}C - ages mentioned in the text are uncalibrated (years before present; y BP) unless otherwise specified (cal BC/ cal AD). Accordingly, Cerro Vicente scoria cone and associated lava flow (Darras et al. 2017) might be the oldest for this period and contemporary to Las Milpillars S (south) lava flow. Subsequently, the massive El Tecolote dome (Fig. 5a) erupted in the south of the area, followed by Las Florecitas, Mesa del Bolsón, and El Caracol lava flows. Las Cabras breached scoria cone (Fig. 5e) and associated debris avalanche and lava flow was dated between $27,395 \pm 390$ and $23,530 \pm 110$ y BP (Fig. 4a, e). Then, Alberca de Guadalupe maar crater erupted $\sim 25,000$ y BP (Siebe et al. 2012) and El Pueblito scoria cone was emplaced between $22,965 \pm 310$ and $21,840 \pm 90$ y BP, Las Pomas dome (Fig. 5f) dated at $19,330 \pm 260$ y BP followed by El Molcajete de Eréndira breached scoria cone (Fig. 5e) dated between $16,319 \pm 300$ and $14,320 \pm 85$ y BP (Fig. 4c, d). Finally, Las Milpillars N (north) lava flow emanated from the small Los Tres Cerritos cones.

During the Holocene, five lava flows were emplaced (each up to ~ 100 m thick). The thick talus deposits at their margins prevented us from reaching paleosols underneath them, with the

exception of El Infiernillo lava flow, which emanated from Las Vigas cone. A date from the paleosol underneath its associated ash fallout layers yielded an age of 3200 ± 30 y BP (Mahgoub et al. 2017b). Stratigraphically, El Infiernillo is the oldest of these Holocene flows. Malpaís Las Víboras and El Capaxtiro directly cover the NW and S lava lobes of El Infiernillo, respectively. Since El Capaxtiro has a less developed soil cover than Malpaís Las Víboras, it must be younger. Mesa La Víbora (to the SW of the study area) has a soil and vegetation cover that is similar to Malpaís Las Víboras; hence, we assumed that they are more or less contemporaneous. Finally, Malpaís Prieto (Fig. 5b, d) is certainly the youngest lava flow in the entire study area, based on by its pitch-black blocky non-vegetated appearance. In a recent study, Mahgoub et al. (2017b) proposed paleomagnetic dates for these lava flows that confirm our proposed chronological sequence: El Infiernillo (1492–1379 BC), Malpaís Las Víboras (1333–1239 and 1024–945 BC), El Capaxtiro (193–84 BC), and Malpaís Prieto (AD 829–962).

Characterization of volcanoes and erupted volumes

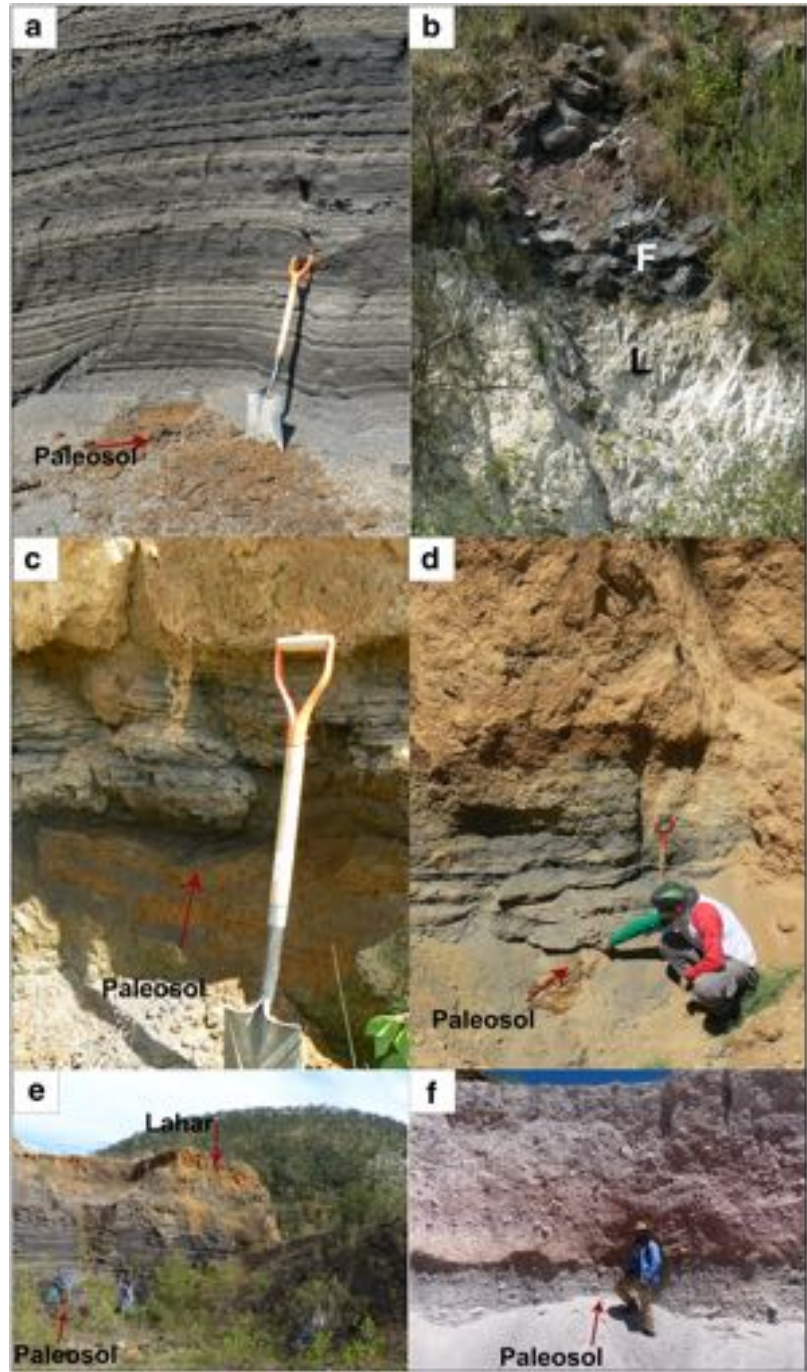
A total of 47 volcanoes were identified in the 395 km^2 mapped area (Fig. 2), where they erupted a total of $\sim 49 \text{ km}^3$ of magma.

Table 2 Radiocarbon dates for monogenetic volcanoes in the western Zacapu basin area, Michoacán. All dates were obtained on paleosols. Note that five samples (laboratory code starting with “A”) were obtained by the conventional method at the University of Arizona by Chris Eastoe. Sample ZAC-12192-A (AA-101151) was also dated at Arizona, but by the accelerator mass spectrometry (AMS) method. The remaining samples (laboratory code starting

with “B”) were obtained at Beta Analytic (Miami, Florida) by the AMS method. Conventional ages were calibrated using Calib 7.1 (Stuiver and Reimer 1993, <http://calib.qub.ac.uk/calib.html>). Half-life used is 5568 years. Asymmetry of errors derives from age calculations involving natural logarithms and is particularly large in small samples with large dilution factors

| Volcano | Sample number | Latitude (N) | Longitude (W) | Altitude (m) | Laboratory code | Conventional age (year BP) | $\delta^{13}\text{C}$ | Calibrated age range 2-sigma (95.4%, CALIB 7.1) | Calibrated age (median probability) (CALIB 7.1) | Deposit dated | Locality | Reference |
|---|---------------|--------------|---------------|--------------|-----------------|----------------------------|-----------------------|---|---|--|------------------------------------|------------|
| Las Vigas scoria cone (El Infernillo lava flow) | ZAC-1524A | 19°51'36.6" | 101°51'08.9" | 2192 m | B-411354 | 3200 +/-30 | -22.2 | cal BP 3366–3470 | cal BP 3420 | Paleosol under ash fallout | 1 km NW of Las Vigas cone | This study |
| Lake deposits below El Capaxtiro lava flow | ZAC-12196-A | 19°49'23.4" | 101°49'09.9" | 2085 m | A-16179 | 13,985 + 245/-235 | -18.9 | cal BP 16261–17,608 | cal BP 16959 | Lacustrine deposit below Capaxtiro lava flow | 2 km W of Zacapu, Zamora | This study |
| Molcayete de Eréndira | ZAC-12192 | 19°49'59.1" | 101°53'34.5" | 2308 m | AA-101151 | 14,320 +/- 85 | -23.5 | cal BP 17150–17,688 | cal BP 17445 | Paleosol under ash fallout | N base of Cerro Cabras | This study |
| Molcayete de Eréndira | ZAC-1054-A | 19°50'29.1" | 101°52'25.4" | 2218 m | A-15494 | 16,935 + 310/-295 | -21.9 | cal BP 19663–21,203 | cal BP 20433 | Paleosol under ash fallout | 2 km N of Eréndira | This study |
| Las Pomas scoria cone | ZAC-1076 | 19°47'23.1" | 101°56'11.5" | 2322 m | A-15493 | 19,330 + 265/-255 | -20.1 | cal BP 22635–23,908 | cal BP 23279 | Paleosol under ash fallout | 3.5 km S of El Pueblito | This study |
| El Pueblito scoria cone | ZAC-14296-A | 19°49'43.1" | 101°55'39.6" | 2365 m | B-378081 | 21,840 +/-90 | -22.3 | cal BP 25863–26,273 | cal BP 26050 | Paleosol under ash fallout | 3.6 km E of Las Cabras cone | This study |
| El Pueblito scoria cone | ZAC-1006B | 19°49'45.0" | 101°55'28.4" | 2451 m | A-15456 | 22,965 + 320/-305 | -23.2 | cal BP 26543–27,735 | cal BP 27239 | Paleosol under ash fallout | N base of El Pueblito scoria cone | This study |
| Las Cabras scoria cone | ZAC-14279 | 19°49'47.0" | 101°53'51.7" | 2324 m | B-378076 | 23,530 +/-110 | -23.1 | cal BP 27476–27,858 | cal BP 27675 | Paleosol under ash fallout | 0.6 km NW of Cabras cone | This study |
| Las Cabras scoria cone | ZAC-14295 | 19°49'23.6" | 101°54'29.2" | 2343 m | B-378080 | 23,570 +/-110 | -21.9 | cal BP 27501–27,885 | cal BP 27700 | Paleosol under ash fallout | 1.6 km WSW of Cabras cone | This study |
| Las Cabras scoria cone | ZAC-14279-X | 19°49'47.0" | 101°53'51.7" | 2324 m | B-378077 | 24,000 +/-110 | -23.3 | cal BP 27764–28,351 | cal BP 28026 | Clayey lahar within ash fallout | A 0.6 km al NW del cono Las Cabras | This study |
| Las Cabras scoria cone | ZAC-14296-P | 19°49'43.1" | 101°55'39.6" | 2365 m | B-378082 | 25,840 +/-110 | -22.3 | cal BP 29625–30,500 | cal BP 30064 | Paleosol under ash fallout | 0.6 km NW of Cabras cone | This study |
| Las Cabras scoria cone | ZAC-12194 | 19°50'00.2" | 101°53'10.5" | 2267 m | A-16177 | 27,395 + 400/-380 | -22.5 | cal BP 30757–32,212 | cal BP 31310 | Paleosol under ash fallout | NE base of Cerro Cabras | This study |

Fig. 4 Examples of typical stratigraphic contexts from which dated materials (mostly paleosols, indicated by arrows) were obtained (localities are shown in Fig. 2 and radiocarbon dates listed in Table 3). **a** Locality ZAC-12194 exposing well-bedded ash and scoria-lapilli fallout from Las Cabras monogenetic cone above paleosol dated at 27,395 + 400/–380 y BP. Shovel is 1 m long. **b** Lake deposits (L) with an exposed thickness of ~3 m underneath El Capaxtiro lava flow (F) at locality ZAC-12196 dated at 13,985 + 245/–235 y BP. **c** Locality ZAC-12192 showing well-bedded fine-ash fallout layers from Molcajete de Eréndira scoria cone above paleosol dated at 14,320 +/- 85 y BP. The paleosol itself developed on top of Las Cabras scoria fallout. **d** Locality ZAC-1054 showing well-bedded ash and scoria-lapilli fallout from Molcajete de Eréndira monogenetic cone above paleosol dated at 16,935 + 310/–295 y BP. **e** Locality ZAC-14279 exposing well-bedded ash and scoria-lapilli fallout (proximal facies) from Las Cabras monogenetic cone (shown in the background) above paleosol dated at 23,530 +/- 110 y BP. Lahar on top (sample ZAC-14279-X) was dated at 24,000 +/- 110 y BP. **f** Pumiceous pyroclastic flow deposits from Las Pomas rhyolite dome that overlie a paleosol dated at 19,330 + 265/–255 y BP at locality ZAC-1076



Of them, nine are Early Pleistocene (~7 km³), 18 Mid-Pleistocene (~26 km³), 15 Late Pleistocene (~11.2 km³), and five Holocene (~4.7 km³) in age. These volumes were calculated using two methods: The first, used only for lava flows, consists of tracing perpendicular elevation profiles along lava flow directions to get an average thickness that is multiplied by the area covered by the flow as obtained using ArcGis 10.1. The second method was applied to domes, cones, and shields.

In this case, the calculation was made in ArcGis 10.1 using the tools “zonal statistics” (to calculate the averaged thickness), “raster calculator” (to determine the number of pixels in a polygon and assign elevation data), and finally “raster calculator as table” (to integrate the number of pixels with elevation data in order to obtain the volume). Because of the unknown variations in void space in the lavas and pyroclastic products of each volcano, we did not recalculate the bulk volume data to dense

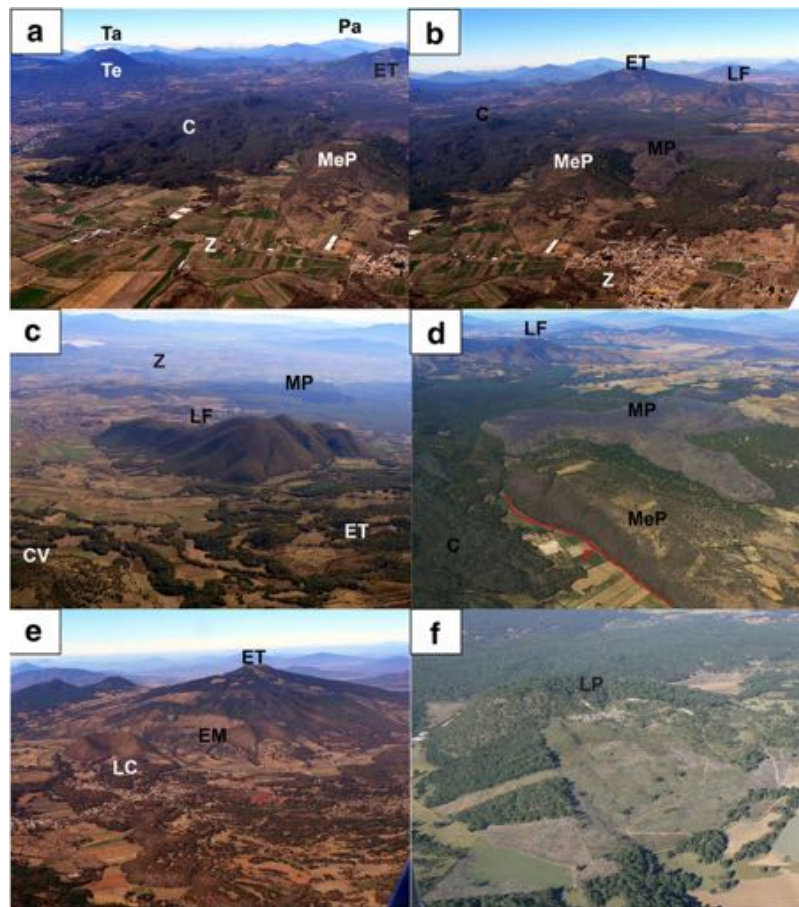


Fig. 5 Diversity of monogenetic volcanic structures in the western Zacapu area. **a** View toward the W showing the Zacapu lacustrine plain (Z), Mesa El Pinal (MeP), and El Capaxtiro (C) lava flows in the foreground. El Tule shield (ET), El Tecolote dome (Te) are in the middle ground, while Tancitaro (Ta) and Patamban (Pa) stratovolcanoes are visible at the horizon. **b** View of the study area to the W. In the foreground is the Zacapu lacustrine plain (Z), in the middle are the Holocene El Capaxtiro (C) and Malpais Prieto (MP) lava flows and Mesa El Pinal (MeP), and in the background El Tule shield (ET) and Las Flores dacite dome complex (LF). **c** View from the WNW toward the Zacapu lacustrine plain (Z). In the foreground are the slopes of the El

Tule shield (ET) and Cerro Vicente (CD), and in the middle ground the Las Flores (LF) dome complex and Malpais Prieto (MP) lava flow. **d** View of the Malpais Prieto lava flow (MP) from the SE. In the foreground are the El Capaxtiro (C) lavas and the Mesa El Pinal (MeP) limited by a steep fault escarpment (F). In the background is the Las Flores dome complex (LF). **e** View of the Las Cabras (LC) and El Molcajete de Eréndira (EM) breached scoria cones from the SE. In the background is El Tule shield (ET). **f** Aerial view of the Las Pomas (LP) rhyolite obsidian dome. Photos taken by Sergio Salinas and Claus Siebe on Feb. 07, 2010 and on Nov. 30, 2011

rock equivalent. Also note that the volume estimates and hence, eruption rates (see below) for rocks older than the Late Pleistocene are minimum values, because of the masking effect due to younger lava flow cover.

In terms of morphological volcano types, the following categories are recognized: 19 thick viscous lava flows, also termed coulées (~40 vol.%), 17 scoria cones with associated lavas (~36 vol.%), seven Mexican shields (~15 vol.%), three domes (~6 vol.%), and one phreatomagmatic tuff cone or maar crater (~2 vol.%). Viscous lava flows and scoria cones with associated lavas were formed during the entire time period (Early Pleistocene to Holocene), shields were emplaced solely during the Early- and Mid-Pleistocene, while domes occur only during the Mid- and Late Pleistocene. A summary

of the morphometric characteristics of volcanoes in the western Zacapu area is presented in Table 3.

Petrography and chemical composition

Ninety-three rock specimens covering all identified volcanoes were collected and analyzed chemically. Only whole-rock compositions are reported here and plotted on a total alkalis ($\text{Na}_2\text{O}+\text{K}_2\text{O}$) vs. SiO_2 diagram (Fig. 6) in order to define magma types. The majority of samples can be classified as andesites, although basaltic andesites and dacites are also common. Rhyolites and alkaline varieties are subordinate, and basalts are notably absent. A map showing the distribution of the different

Table 3 Summary of the morphometric characteristics of volcanoes in the western Zacapu basin area. Volcanoes are listed in decreasing age. Asterisks (*) denote volcanoes whose products extend beyond the limits of the mapped quadrangle and degree signs (°) denote lava flows directly associated to a scoria cone

| Volcano | Composition | Volcano type | Average thickness (km) | Area (km ²) | Volume (km ³) | Volume of the cone (km ³) | Total volume (km ³) | Eruption rate (km ³ /ka) |
|-------------------------------|-------------------------|------------------------|------------------------|-------------------------|---------------------------|---------------------------------------|---------------------------------|-------------------------------------|
| Early Pleistocene (2–1 Ma) | | | | | | | | |
| La Guajolota* | Dacite | Lava flow | – | 11.7 | 1.1 | – | 1.1 | |
| Mesa El Pinal | Andesite | Lava flow | 0.14 | 3.7 | 0.51 | – | 0.5 | |
| Brinco del Diablo* | Trachy-andesitic basalt | Shield | – | 7.0 | 1.40 | – | 1.4 | |
| Cuinato | Andesite | Lava flow | 0.04 | 1.2 | 0.05 | – | 0.0 | |
| El Pinal* | Andesite | Lava flow | – | 6.4 | 0.57 | – | 0.6 | |
| El Agostadero* | Andesite | Shield | – | 1.9 | 0.27 | – | 0.3 | |
| El Cuije* | Andesite | Shield | – | 5.8 | 0.93 | – | 0.9 | |
| Tzantzán | Andesite | Lava flow | – | 4.4 | 0.47 | – | 0.5 | |
| El Fresno* | Andesite | Shield | – | 9.6 | 1.70 | – | 1.7 | |
| | | | | | | Subtotal | 7.0 | 0.007 |
| Mid-Pleistocene (1 Ma–100 ka) | | | | | | | | |
| | Andesite | Lava flow [°] | 0.01 | 1.7 | 0.02 | 0.028 | 0.05 | |
| Flujo Sin Nombre | Andesite | Lava flow [°] | 0.04 | 5.0 | 0.19 | 0.062 | 0.25 | |
| Las Flores | Dacite | Dome complex | – | 8.8 | 2.04 | – | 2.04 | |
| Las Minas | Dacite | Lava flow | 0.06 | 2.2 | 0.14 | – | 0.14 | |
| Los Espinos | Andesite | Lava flow | 0.06 | 5.8 | 0.32 | – | 0.32 | |
| El Llano | Andesite | Lava flow | 0.02 | 3.8 | 0.08 | – | 0.08 | |
| San Antonio Tariácuri | Andesite | Lava flow | 0.03 | 2.7 | 0.07 | – | 0.07 | |
| Santa Gertrúdis | Andesite | Lava flow | 0.01 | 2.3 | 0.02 | – | 0.02 | |
| Loma Marijo | Andesite | Lava flow | 0.00 | 0.7 | 0.00 | – | 0.00 | |
| El Copalillo-C. Pelón | Andesite | Lava flow [°] | 0.10 | 21.5 | 2.22 | 0.99 | 3.20 | |
| En Medio* | Andesite | Lava flow [°] | – | 9.7 | 0.10 | 0.02 | 0.12 | |
| El Molcajetito | Andesite | Lava flow [°] | 0.03 | 0.5 | 0.02 | 0.06 | 0.08 | |
| Flujo Sin Nombre VI | Andesite | Lava flow [°] | 0.04 | 1.2 | 0.04 | – | 0.04 | |
| El Coyotillo-El Durazno | Andesite | Lava flow [°] | 0.04 | 5.0 | 0.20 | 0.07 | 0.27 | |
| Mesa Piritzio* | Andesite | Lava flow | 0.08 | 7.5 | 0.58 | – | 0.58 | |
| De En Medio* | Andesite | Shield | – | 7.8 | 0.21 | – | 0.21 | |
| El Tule* | Andesite | Shield | – | 53.5 | 18.01 | – | 18.01 | |
| Picacho* | Andesite | Shield | – | 1.8 | 0.50 | – | 0.50 | |
| | | | | | | Subtotal | 26.0 | 0.03 |
| Late Pleistocene (100–11 ka) | | | | | | | | |
| Alberca de Los Espinos | Andesite | Maar | – | 1.6 | 0.40 | – | 0.40 | |
| C. Vicente | Dacite | Lava flow [°] | 0.07 | 8.6 | 0.58 | 0.09 | 0.67 | |
| Las Milpillas S | Dacite | Lava flow [°] | 0.02 | 1.8 | 0.04 | 0.07 | 0.11 | |
| El Tecolote* | Andesite | Dome | – | 29.3 | 7.30 | – | 7.30 | |
| Las Florecitas | Andesite | Lava flow [°] | 0.04 | 2.3 | 0.08 | 0.06 | 0.14 | |
| Los Hornos* | Andesite | Lava flow [°] | – | 1.3 | 0.06 | – | 0.06 | |
| Mesa del Bolsón | Andesite | Lava flow | 0.08 | 1.8 | 0.14 | – | 0.14 | |
| El Caracol | Andesite | Lava flow | 0.09 | 3.9 | 0.36 | – | 0.36 | |
| Las Cabras | Andesite | Lava flow [°] | – | 18.8 | 0.60 | 0.1 | 0.70 | |
| Cercano a Las Pomas* | Andesite | Lava flow [°] | 0.05 | 3.8 | 0.18 | – | 0.18 | |
| El Pueblito | Basaltic andesite | Lava flow [°] | 0.06 | 7.5 | 0.45 | 0.08 | 0.53 | |
| Las Pomas | Rhyolite | Dome | – | 1.5 | 0.14 | – | 0.14 | |
| El Molcajete de Eréndira | Basaltic andesite | Lava flow [°] | 0.07 | 1.3 | 0.09 | 0.03 | 0.13 | |
| Las Milpillas N | Basaltic andesite | Lava flow [°] | 0.17 | 1.3 | 0.23 | 0.01 | 0.24 | |

Table 3 (continued)

| Volcano | Composition | Volcano type | Average thickness (km) | Area (km ²) | Volume (km ³) | Volume of the cone (km ³) | Total volume (km ³) | Eruption rate (km ³ /ka) |
|---------------------|-------------------|------------------------|------------------------|-------------------------|---------------------------|---------------------------------------|---------------------------------|-------------------------------------|
| C. La Arena* | Basaltic andesite | Lava flow | – | 1.4 | 0.10 | – | 0.10 | |
| | | | | | | Subtotal | 11.2 | 0.13 |
| Holocene (11–0 ka) | | | | | | | | |
| El Infiernillo | Andesite | Lava flow ^o | 0.05 | 5.8 | 0.29 | 0.01 | 0.29 | |
| Malpaís Las Víboras | Andesite | Lava flow | 0.08 | 5.9 | 0.47 | – | 0.47 | |
| Mesa La Víbora | Andesite | Lava flow | 0.10 | 2.5 | 0.25 | – | 0.25 | |
| El Capaxtiro | Andesite | Lava flow complex | 0.15 | 20.9 | 3.13 | 0.02 | 3.16 | |
| Malpaís Prieto | Andesite | Lava flow | 0.09 | 5.7 | 0.51 | – | 0.51 | |
| | | | | | | Subtotal | 4.68 | 0.44 |
| | | | | | | Total | 48.9 | |

rock types is shown in Fig. 7. Andesite is by far the most voluminous product with 42 km³ (86 vol.%) followed by 4 km³ of dacite (8 vol.%), 1.4 km³ of basaltic trachy-andesite (3 vol.%), 1 km³ of basaltic andesite (2 vol.%), and only 0.14 km³ of rhyolite (0.3 vol.%). Although few single volcanoes show a chemical transition (e.g., from basaltic andesite to andesite) in their products, their composition is in general quite homogeneous with SiO₂ variations being < 2 wt.%.

Thin sections of 75 rock samples were analyzed under the petrographic microscope in order to obtain their modal (1000 points counted) mineralogical composition (Reyes-Guzmán 2017). The basaltic andesite group (Fig. 8a) typically shows irregular to elongated vesicles (3.7–62.5 vol.%) up to 2.5 mm in size, with phenocrysts (0.3–5.3 vol.%) of olivine (0.1–

1.5 vol.%), plagioclase (0.2–3.2 vol.%), augite (0.1–0.3 vol.%), and occasional hypersthene (0.3 vol.%). Microphenocrysts (0.9–26.4 vol.%) include plagioclase, augite, and hypersthene. The matrix (18.6–75.4 vol.%) consists of microlites and glass. The andesite group is formed by rocks with a porphyritic texture and phenocrysts (< 10 vol.%) in a microlitic (17–73.7 vol.%) to glassy (4.3–48.6 vol.%) matrix. Vesicles are mainly elongated (< 2 mm) and up to 33 vol.%. The phenocrysts include augite (< 1.8 vol.%) and hypersthene (< 4 vol.%), occasionally forming together glomeroporphyritic clusters (Fig. 8b), plagioclase (< 7.4 vol.%), and opacitized hornblende (1.5 vol.%; Fig. 8c). Although quartz xenocrysts surrounded by a reaction corona of augite microlites (Fig. 8d) and phenocrysts of plagioclase displaying

Fig. 6 Whole-rock composition of volcanic products classified by age (colors denote same age groups as shown on map in Fig. 2). Limits of fields after Le Maitre (2002). Data was normalized to 100% on anhydrous basis

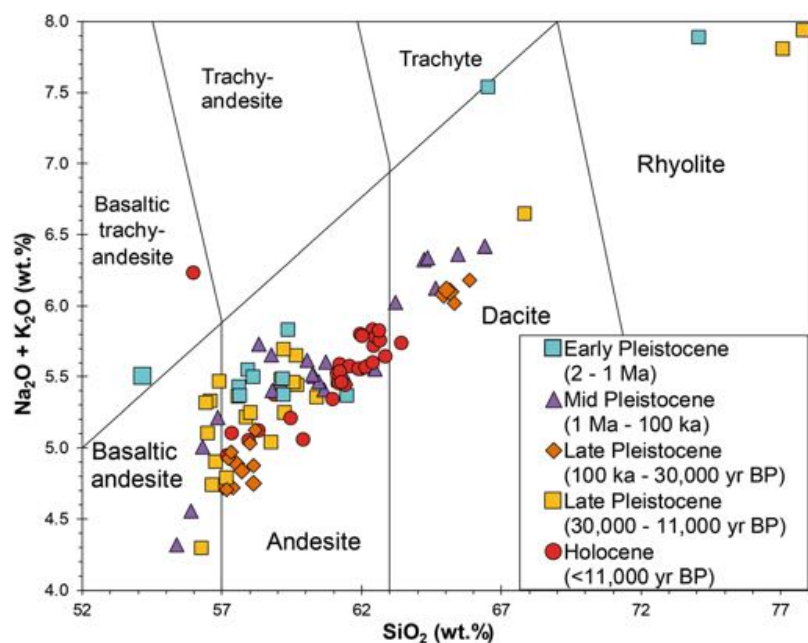
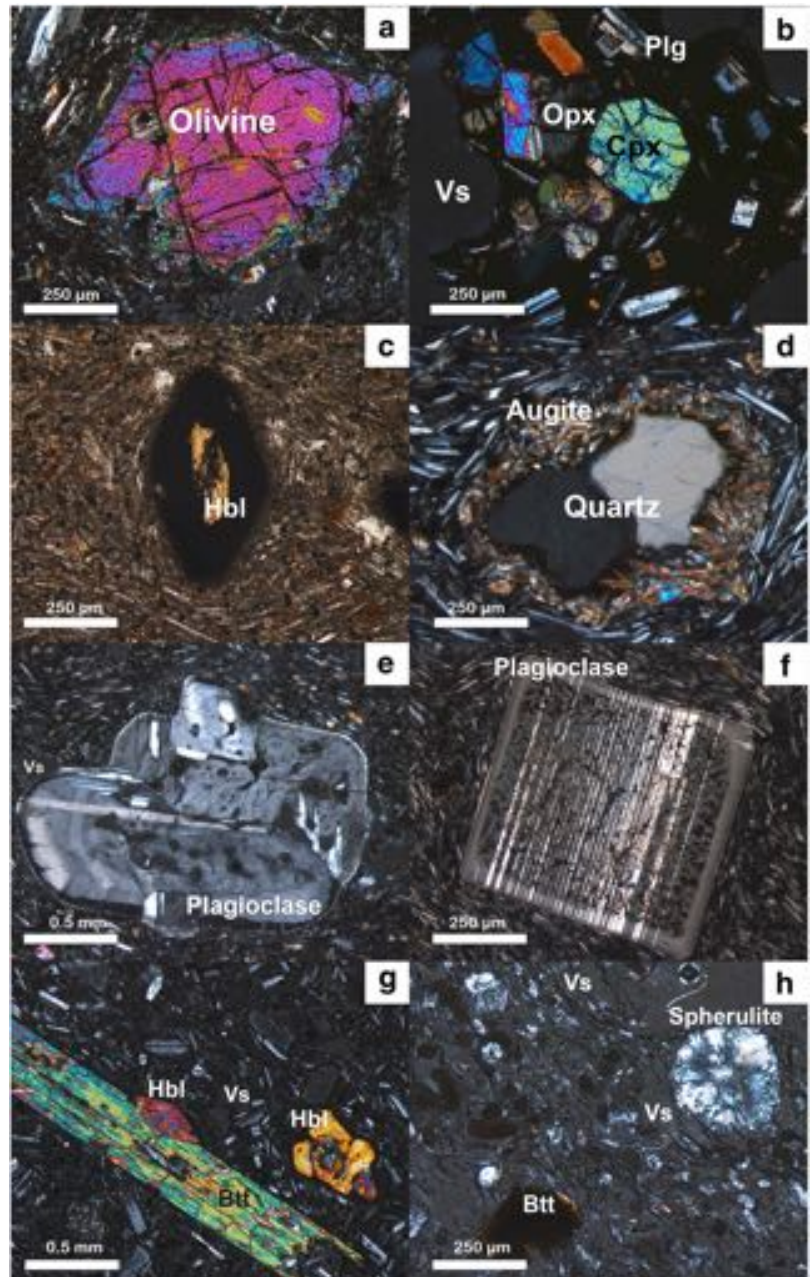


Fig. 8 Photomicrographs of typical rock types in the study area taken under the petrographic microscope (crossed nicols). **a** Basaltic andesite (ZAC-1013) from El Infiernillo lava flow (Cerro Las Vigas scoria cone) showing an idiomorphic olivine crystal in a glassy matrix with abundant microlites. **b** Andesite from El Tule shield (ZAC-1004) containing a glomero-porphyrific clusters of augite (Cpx) and hypersthene (Opx) crystals in a glassy matrix. Vs = vesicle. **c** Andesite (ZAC-1509) from the Malpaís Prieto lava flow displaying a strongly opacitized hornblende crystal. **d** Andesite from Cerro Cuinato (ZAC-1536) showing two quartz xenocrysts surrounded by a reaction corona of augite microlites. **e** Andesite from El Molcajetito scoria cone (ZAC-1056) showing a resorbed and zoned plagioclase crystal with a sieved texture and polysynthetic twinning. **f** Dacite from Las Milpillas lava flow (ZAC-1520) showing a plagioclase xenocryst with polysynthetic twinning and a sieved texture. **g** Dacite from Las Flores dome (ZAC-1536) with biotite (Bt) and hornblende (Hbl) crystals in a glassy matrix with abundant feldspar microlites and vesicles (vs). **h** Rhyolite from Las Pomas dome (ZAC-1546) displaying opacitized biotite crystals and micro-spherulites in a glassy microvesicular matrix



lacustrine basin only Quaternary rocks (<2.1 Ma) are exposed due to the high frequency of eruptions and dense cover of young volcanic products. Erupted rocks are mainly andesites devoid of xenoliths. However, xenocrysts observed under the microscope in several Holocene lava flows (e.g., plagioclase displaying polysynthetic twinning and sieved textures and quartz with reaction coronas of augite) point toward the possible existence of a crystalline basement, as previously suggested by Corona-Chávez et al. (2006) to occur underneath the Arocutin scoria cone at the shores of nearby lake Pátzcuaro. Such basement might consist of Tertiary

granodiorites, as observable at the southern margin of the MGVF near Jorullo volcano (Guilbaud et al. 2011).

The relative proportions of the different magma types erupted do not vary systematically through time (Fig. 9). Andesites were erupted constantly during the entire last 2.1 Ma and their erupted volume does not show clear variations, while the erupted volume of dacites decreased systematically since its peak in the Early Pleistocene. In contrast, basaltic andesite eruptions are subordinate and only became more frequent in the Late Pleistocene. Rhyolite is almost negligible (only one eruption during the Late Pleistocene forming

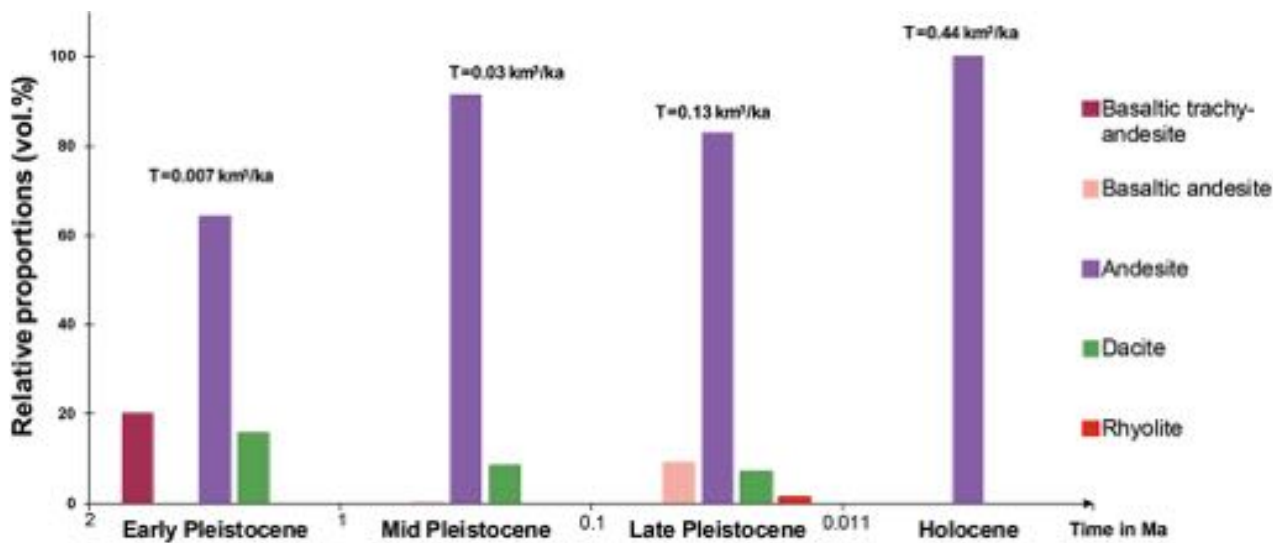


Fig. 9 Variation of the proportions of volcanic rock types with time over the last 2 Ma. T = erupted rate. Note that values for the Pleistocene are minimum due to coverage by younger products. Colors denote same rock types as shown on map in Fig. 7

the small Las Pomás dome) and basaltic trachy-andesite was also erupted only once in the Early Pleistocene forming the voluminous El Brinco del Diablo shield.

Estimated minimum eruption rates (km^3/ka) for the different time periods are 0.007 for the Early Pleistocene, 0.03 for the Mid-Pleistocene, 0.13 for the Late Pleistocene, and $0.44 \text{ km}^3/\text{ka}$ for the Holocene (Table 3). In comparison to the eruption rate of $0.2 \text{ km}^3/\text{ka}$ reported by Hasenaka (1994) for the entire MGVF for the period between 3 and 1 Ma, the eruption rate in the study area is relatively low ($0.007 \text{ km}^3/\text{ka}$). For the last one million years, Hasenaka (1994) reported an eruption rate of $0.7 \text{ km}^3/\text{ka}$ for the entire MGVF, while in the study area the rate is $0.04 \text{ km}^3/\text{ka}$. On the other hand, Guilbaud et al. (2012) reported an eruption rate of $> 0.017 \text{ km}^3/\text{ka}$ for the Tacámbaro-Puruarán area (located 55 km to the S of Zacapu) for the last one million years. They also reported an eruption rate of 0.34 to $0.39 \text{ km}^3/\text{ka}$ for the Holocene, which is similar to the one reported here for the western Zacapu basin ($0.44 \text{ km}^3/\text{ka}$). Furthermore, in the study area more voluminous shields formed during the Mid-Pleistocene than in the Late Pleistocene. Overall, volcanism is effusive in most cases with the prevalence of lava flows and the eruption rates can be considered normal in the context of the entire MGVF, but much higher than normal for the Holocene.

Most vents (especially scoria cones) are typically aligned NE-SW to ENE-WSW (CFS-direction; Figs. 1, 2). Andesites occur throughout the area, but dacites form a cluster and seem to be aligned along a NNW-SSE chain, oblique to the general trend, starting in the NW with the Early Pleistocene La Guajolota and ending with the Late Pleistocene Las Milpillás S flow to the SE in the central part of the study area (Fig. 7). In the case of the basaltic andesites, their alignment is

not as clear as for the dacites, but they seem to follow the dominant NE-SW to ENE-WSW direction. The only isolated rhyolite (Las Pomás) is in the SW and the single basaltic trachy-andesite (Brinco del Diablo) in the NE corner of the study area, respectively (Fig. 7). Early Pleistocene volcanoes (Fig. 2) tend to be aligned along a single ENE-WSW trend in the northern part of the quadrangle, while the Mid-Pleistocene volcanoes follow the same direction but further SE in the central part of the study area. The Early Pleistocene and Holocene structures are equally aligned ENE-WSW, but again shifted to the SE with respect to the older structures. In short, a progressive shift of vents toward the margin of the lake is clear, implying that the younger lavas displaced the lakeshore. As a result, older lake deposits were covered and directly underlie the youngest lavas, as observable at several outcrops (Fig. 4b) along the road west of Zacapu city (Fig. 2).

A closer look at the volcanoes emplaced during the past 30,000 years reveals that they all occur along a narrow 2-km-wide ENE-WSW stripe that diagonally crosses the study area (Fig. 2). Furthermore, their eruptions did not occur at regular time intervals, but in a clustered fashion during two different periods (see time graph in Fig. 10). The first cluster includes four volcanoes and initiated $\sim 27,000 \text{ BC}$ with the eruption of Alberca de los Espinos tuff cone, shortly before the Last Glacial Maximum. This cluster lasts for almost 6000 years until $\sim 21,300 \text{ BC}$ with the eruption of the Las Pomás rhyolite dome. After a hiatus of ~ 5000 years, the small volume El Molcajete de Eréndira ($\sim 16,000 \text{ BC}$) eruption occurs, followed again by a long hiatus in activity of $\sim 11,000$ years, until the second cluster initiates with the eruption of Las Vigas basaltic andesite scoria cone (El Infiernillo lava flow) at $\sim 1470 \text{ BC}$. The last eruption in this cluster is the high-silica andesitic Malpaís Prieto lava flow at $\sim \text{AD } 900$. This second cluster is

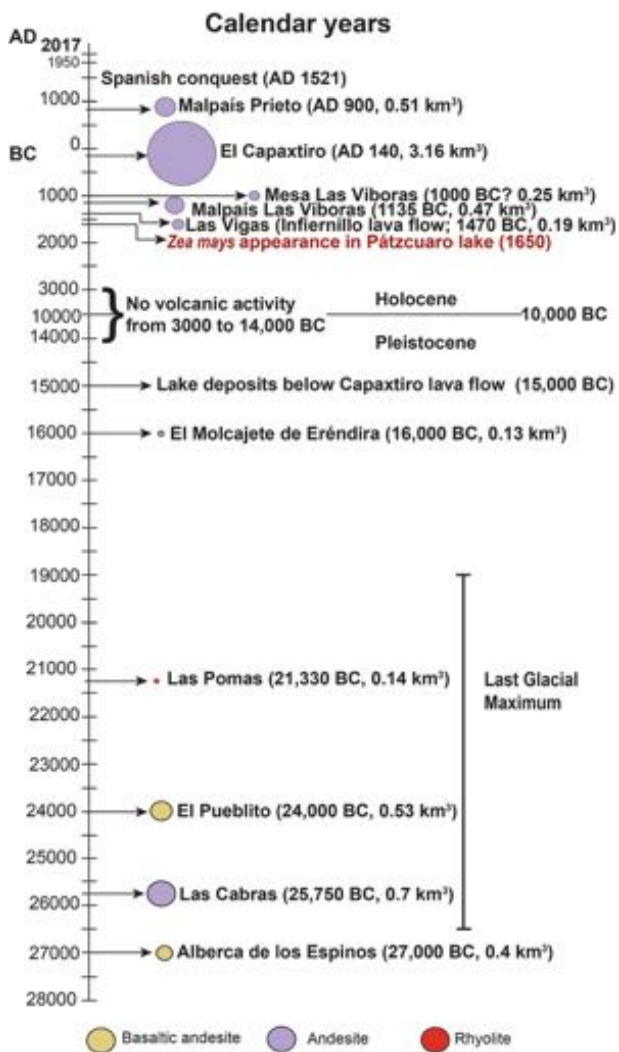


Fig. 10 Time graph showing the age (calibrated dates in calendar years), composition, and volume of eruptions in the western Zacapu basin area for the past 30,000 years. Dates for the Holocene Malpaís Prieto, El Capaxtiro, and Malpaís Las Viboras lava flows were obtained by the paleomagnetic method by Mahgoub et al. (2017b), the date for Alberca de Los Espinos is from Siebe et al. (2012), the date for *Zea mays* pollen in lake Pátzcuaro is from Watts and Bradbury (1982), and the time range for the Last Glacial Maximum is from Clark et al. (2009)

much more restricted in time (five volcanoes erupted in a time interval of only 2500 years), and in space (most vents are less than 3 km apart from each other), but also in composition (mostly andesites). Furthermore, in the southern area of this cluster, the preexisting lake deposits dated at ~14,000 y BP (Table 1, Fig. 4b) were upheaved by ~100 m, as attested by their elevation (~2080 m asl) with respect to all the remaining areas with such deposits around the lake basin (~1980 m asl). The single occurrence of lake deposits at such a high position rules out the possibility of them representing a former high-water mark of the lake level. Since the upheaved lake deposits are overlain by El Capaxtiro's southern lava flows, we

speculate that the El Capaxtiro eruption was preceded/ accompanied by some sort of shallow laccolithic intrusion, maybe at the base of the low-density lacustrine sequence.

The identification of such small clusters comprising several monogenetic volcanoes of differing compositions that erupted over geologically brief time intervals (several thousands of years) in small areas within the wider MGVF leads to important questions in regard to future volcanic hazard assessments in this region: Is the Holocene cluster north of the city of Zacapu still potentially active: the last eruption occurred only ~1100 years ago. Should a new eruption be expected in the near future? Will the next monogenetic eruption in the MGVF be a single short-lived isolated eruption, or the beginning of a new cluster? Furthermore, should the historic eruptions of Jorullo and Parícutin be envisaged as single isolated eruptions or is it possible that each of them represents the beginning of a cluster? Hence, should a new eruption in their close vicinity be expected in the future? At this point, all of these questions are unanswerable but the relevance of clustered monogenetic volcanism in a subduction-related volcanic arc is further underscored by the fact that the cases described here are not unique. A similar Holocene cluster (four vents ranging from 3800 to 400 BC, basaltic andesites to high-silica andesites) was recently reported from the Tacámbaro area (Guilbaud et al. 2012; Mahgoub et al. 2017c) in the southern part of the MGVF. Deligne et al. (2016) describe a cluster of basaltic eruptions of different compositions from central OR, USA. In both of these examples, several different magma sources were tapped over short periods. The causes that lead to the formation of multiple magma sources and the spatial concentration of volcanic activity need to be addressed in order to evaluate the potential impacts of clustered volcanism in the MGVF and elsewhere. Future work, especially geophysical and petrological studies are needed to elucidate the conditions that allow several magma sources to be formed and then tapped in close temporal and spatial proximity.

Another observation is the frequent occurrence of monogenetic andesite lava flows (e.g., Malpaís Prieto), whose emplacement was purely effusive and not preceded nor accompanied by violent Strombolian explosive activity and the formation of a scoria cone and associated ash fallout (as in the historic example of Parícutin described by Luhr and Simkin 1993). Solely effusive andesite eruptions require that magmas feeding them, rise slowly or stagnate at low pressures during their final ascent in the upper crust in order to allow substantial gas-loss prior to eruption (see Chevrel et al. 2016b). The latter puts further constraints on the framework of the magmatic plumbing system feeding monogenetic eruptions and its understanding is crucial for developing strategies aimed at reducing risk in the active MGVF, and in particular in the municipality of Zacapu, inhabited today by >75,000 people (INEGI 2016).

Implications for archeology

The Zacapu lacustrine basin has a total catchment area of 1480 km² including the surrounding volcanic highlands (Kshirsagar et al. 2015). Its lowest part (1980 m asl) was occupied by a broad (~260 km²) but shallow (~30 m) lake which possessed a small natural discharge toward the north (Siebe et al. 2012) until it was artificially drained in the late nineteenth century to gain fertile land for agricultural purposes (Noriega and Noriega 1923). Before being drained, the lake environment and its resources (e.g., fish, amphibians, waterfowl, aquatic plants) played an important role for the people living in towns at its shores. The availability of water and diversity of food sources were attractive to early nomads and a key factor in promoting the transition to sedentary life and permanent human settlement in prehistoric times (e.g., Pétrequin 1994). During the time of early human occupation, the Late Holocene El Infiernillo (cal 1525-1420 BC), Malpaís Las Víboras (~1200 BC), and El Capaxtiro (~150 BC) lava flows were emplaced (Mahgoub et al. 2017b). The zones immediately surrounding the lavas probably remained deserted for some time because of the fear provoked by earthquakes and noises directly associated to the eruptions. Archeological investigations in the Zacapu area since the early 1980s (Michelet 1992; Michelet et al. 1989) have revealed that the human occupation of these young lava flows started ~100 BC during the late Preclassic period of Mesoamerican archeology, probably shortly after El Capaxtiro eruption (Mahgoub et al. 2017b). The population density increased and was continuous as of AD 550 until abandonment of the entire area occurred around AD 900 (late to terminal Classic): this coincides with the Malpaís Prieto eruption (Mahgoub et al. 2017b). Interestingly, this area was heavily repopulated again only few hundred years later around AD 1250 and belongs to the core region in which the Tarascan civilization has its roots, as described in the *Relación de Michoacán*, an ethno-historic document compiled from oral traditions in 1541 by the Franciscan friar Jerónimo de Alcalá (De Alcalá 2000). Surface morphology studies and analysis of a high-resolution LIDAR image carried out under the umbrella of the Uacusecha archeological project, both indicate that the El Infiernillo, El Capaxtiro, and Malpaís Prieto lava flows were occupied by four large urban settlements during the middle/late Preclassic (AD 1250–1450). The ruins of thousands of domestic units as well as 50 ceremonial complexes with temple mounds are still observable (Michelet 1998; Migeon 1998; Forest 2014; Pereira et al. 2017 in press). The apparently inhospitable rocky substrate devoid of soil and vegetation not withstanding these young lava flows became a densely populated dwelling hub. We speculate that the rough lava flows became attractive as a dwelling ground precisely because of some of their most notable geologic features: They represented secure natural clearings within an otherwise

densely forested area prone to periodic wildfires, frequent during the dry season. In addition, heavy building material for fences and walls was readily available in the form of loose blocks. The steep marginal levees of the lava flows may have served as a natural fortification. Also, the occupation of the rocky substrate by houses and public buildings would optimize land use by maximizing the availability of fertile soil surfaces for agricultural purposes, augmenting crop yields. Finally, walking distances to the lake shore to the east and its resources are less than an hour, and rock types such as glassy dacites suitable for the manufacture of cutting tools (Darras et al. 2017) are available in close vicinity at Las Minas and Cerro Vicente lava flows (Fig. 2). In conclusion, it seems that in terms of human development, the recent volcanic activity in the western Zacapu basin, brought far more benefits than drawbacks, especially since it occurred in conjunction with a rich and diverse lake environment under favorable climate conditions. Future archeological excavations should reveal additional interesting facts that will shed light on the intricacies of all of these environmental factors and their respective roles in the development of ancient societies and their migrations in this region.

Conclusions

Geological mapping of a 395 km²-sized quadrangle encompassing the western margin of the Zacapu lacustrine basin in the north-central part of the Michoacán-Guanajuato volcanic field allowed identifying a total of 47 monogenetic volcanoes. These include 19 viscous lava flows, 17 scoria cones with associated lava flows, seven lava shields, three domes, and one phreatomagmatic maar. Erupted products are mostly effusive and dominantly andesites with 42 km³ followed by 4 km³ of dacite, 1.4 km³ of basaltic trachy-andesite, 1 km³ of basaltic andesite, and 0.14 km³ of rhyolite, while basalts are notably absent. Eruptive centers are commonly aligned ENE-WSW following the direction of the regional seismically active Cuitzeo Fault System.

⁴⁰Ar/³⁹Ar and ¹⁴C radiometric dating revealed that the great majority of volcanic rocks is younger than ~2.1 Ma and that activity migrated toward the SE. Estimated minimum eruption rates (km³/ka) for the different time periods are 0.007 for the Early Pleistocene, 0.03 for the Mid-Pleistocene, 0.13 for the Late Pleistocene, and 0.44 for the Holocene. Of these, the rate for the Holocene is relatively high and comparable in magnitude to the rate reported for the Tacámbaro-Puruarán area in the southern part of the MGVF.

In the past 30,000 years, eruptions occurred along a narrow 2-km-wide and 25-km-long, ENE-WSW oriented stripe, and were clustered during two main time periods. The first cluster (27,000–21,300 BC) includes four volcanoes. After a period of almost 20,000 years, with only one eruption (El Molcajete

de Eréndira, ~ 16,000 BC), the second cluster (1479–900 BC) of five eruptions initiates with the eruption of Las Vigas basaltic andesite scoria cone (El Infiernillo lava flow) and ends with the high-silica andesitic Malpaís Prieto lava flow at ~ AD 900. This second cluster is more restricted in space: most vents are < 3 km apart from each other.

Lacustrine basins in central Mexico were attractive to early human occupation. Recent archeological investigations have documented that the human occupation history of these young lava flows started ~ 100 BC during the late Preclassic period of Mesoamerican archeology, probably shortly after El Capaxtiro eruption. Population became denser and was continuous as of AD 550 until an abandonment of the entire area occurred around AD 900 (late to terminal Classic), which coincides with Malpaís Prieto eruption, suggesting a causal link. In spite of their apparently inhospitable appearance, El Infiernillo, El Capaxtiro, and Malpaís Prieto lava flows became heavily repopulated again only few hundred years later ~ AD 1250. We speculate that the barren and rough lava flows were attractive because they provided building material for walls and fences, and security against wildfires and enemies. It seems that the recent volcanic activity in the western Zacapu basin brought not only risks, but also many benefits to human development, especially since it occurred in conjunction with a rich and diverse lake environment under favorable climate conditions.

Acknowledgments Archeologists G. Pereira and O. Quezada kindly provided archeological information and showed us their excavation sites in the Zacapu area. P. Kshirsagar allowed us the use of her wonderful map of the MGVF. We thank Américo González-Esparza, Adriana Briseño, and Ernesto Andrade at UNAM Campus Morelia for providing lodging facilities at the Mexican Array Radio Telescope (MEXART) near Coeneo during field campaigns. Capitán Fernando Valencia is thanked for skillful and safe flights over the study area. Two anonymous reviewers and journal editor Richard J. Brown were very helpful and we are thankful for their constructive criticism and valuable suggestions.

Funding information Field and laboratory costs were defrayed from projects funded by Consejo Nacional de Ciencia y Tecnología (CONACyT-167231) and the Dirección General de Asuntos del Personal Académico (DGAPA-UNAM-IN101915, IN113517) granted to C. Siebe and M.N. Guilbaud. M.O. Chevrel was funded by a UNAM-DGAPA postdoctoral fellowship (2014-2016).

References

Agustín-Flores J, Siebe C, Guilbaud M-N (2011) Geology and geochemistry of Pelagatos, Cerro del Agua, and Dos Cerros monogenetic volcanoes in the Sierra Chichinautzin volcanic field, south of Mexico City. *J Volcanol Geotherm Res* 201(1-4):143–162. <https://doi.org/10.1016/j.jvolgeores.2010.08.010>

Ban M, Hasenaka T, Delgado-Granados H, Takoaka N (1992) K-Ar ages of lavas from shield volcanoes in the Michoacán-Guanajuato volcanic field, Mexico. *Geofis Int* 31:467–473

Blatter DL, Hammersley L (2010) Impact of the Orozco Fracture Zone on the central Mexican Volcanic Belt. *J Volcanol Geotherm Res* 197(1-4):67–84. <https://doi.org/10.1016/j.jvolgeores.2009.08.002>

Carmichael ISE (2002) The andesite aqueduct: perspectives on the evolution of the intermediate magmatism in west-central (105°–99°W) Mexico. *Contrib Mineral Petrol* 143(6):641–663. <https://doi.org/10.1007/s00410-002-0370-9>

Chevrel MO, Siebe C, Guilbaud M-N, Salinas S (2016a) The AD 1250 El Metate shield volcano (Michoacán): Mexico's most voluminous Holocene eruption and its significance for archeology and hazards. *The Holocene* 26(3):471–488. <https://doi.org/10.1177/0959683615609757>

Chevrel MO, Guilbaud M-N, Siebe C (2016b) The ~AD 1250 effusive eruption of El Metate shield volcano (Michoacán, México): magma source, crustal storage, eruptive dynamics, and lava rheology. *Bull Volcanol* 78:1–28. <https://doi.org/10.1007/s00445-016-1020-9>

Clark PU, Dyke AS, Shakun JD, Carlson AE, Clark J, Wohlfarth B, Mitrovica JX, Hostetler SW, McCabe AM (2009) The last glacial maximum. *Science* 325(5941):710–714. <https://doi.org/10.1126/science.1172873>

Corona-Chávez P, Reyes-Salas M, Garduño-Monroy VH, Israde-Alcántara I, Lozano-Santa Cruz R, Morton-Bermea O, Hernández-Álvarez E (2006) Asimilación de xenolitos graníticos en el Campo Volcánico Michoacán-Guanajuato: el caso de Arócutin Michoacán, México. *Rev Mex Cienc Geol* 23(2):233–245

Darras V, Mireles C, Siebe C, Quezada O, Castañeda A, Reyes-Guzmán N (2017) The other stone. Dacite quarries and workshops in the prehispanic Tarascan Territory, Michoacán, Mexico. *J Archeol Sci Rep* 12:219–231. <https://doi.org/10.1016/j.jasrep.2017.01.034>

De Alcalá FJ (2000 [1541]) Relación de Michoacán, o, relación de las ceremonias y ritos y población y gobernación de los indios de la Provincia de Mechuacán. (Introductory study and edition by Moisés Franco Mendoza). El Colegio de Michoacán, Zamora. 128 pp

Deligne NI, Conrey RM, Cashman KV, Champion DE, Amidon WH (2016) Holocene volcanism of the upper McKenzie River catchment, central Oregon Cascades, USA. *Bull Geol Soc Am* 128(11/12):1618–1635. <https://doi.org/10.1130/B31405.1>

Demant A (1978) Características del Eje Neovolcánico Transmexicano y sus problemas de interpretación. *Rev Mex Cienc Geol* 2(2):172–187

Demant A (1992) Marco geológico regional de la laguna de Zacapu, Michoacán, México. In: Demant A, Labat JN, Michelet D, Tricart J (eds) El Proyecto Michoacán 1983–1987. Medio Ambiente e Introducción a los Trabajos Arqueológicos. CEMCA, México, D.F. Collection Etudes Mésoaméricaines II-11, pp 53–72

Fisher CT, Leisz SJ (2013) New perspectives on Purépecha urbanism through the use of LiDAR at the site of Angamuco. In: Comer DC, Harrower MJ (eds) Mapping archaeological landscapes from space. Springer briefs in archaeology. pp 199–210

Fisher CT, Cohen AS, Fernández-Díaz JC, Leisz SJ (2017) The application of airborne mapping LiDAR for the documentation of ancient cities and regions in tropical regions. *Quat Int* 448:129–138. <https://doi.org/10.1016/j.quaint.2016.08.050>

Forest M (2014) Approches spatio-archéologiques de la structure sociale des sites urbains du Malpaís de Zacapu. PhD dissertation, Université de Paris 1 – Panthéon/Sorbonne, Paris

García-Cook A (2003) Cantona: the city. In: Sanders WT, Mastache AG, Cobean RH (eds) Urbanism in Mesoamerica Vol. 1, Instituto Nacional de Antropología e Historia and Pennsylvania State University, pp 311–344

Garduño-Monroy VH, Pérez-López R, Israde-Alcántara I, Rodríguez-Pascua MA, Szykaruk E, Hernández-Madrigal VM, García-Zepeda ML, Corona-Chávez P, Ostroumov M, Medina-Vega VH, García Estrada G, Carranza O, López-Granados E, Mora-Chaparro JC (2009) Paleoseismology of the southwestern Morelia-Acambay fault system, central Mexico. *Geofis Int* 48(3):319–335

- Guilbaud M-N, Siebe C, Layer P, Salinas S, Castro-Govea R, Garduño-Monroy VH, Corvec NL (2011) Geology, geochronology, and tectonic setting of the Jurullo Volcano region, Michoacán, México. *J Volcanol Geotherm Res* 201(1-4):97–112. <https://doi.org/10.1016/j.jvolgeores.2010.09.005>
- Guilbaud M-N, Siebe C, Layer P, Salinas S (2012) Reconstruction of the volcanic history of the Tacámbaro-Puruarán area (Michoacán, México) reveals high frequency of Holocene monogenetic eruptions. *Bull Volcanol* 74(5):1187–1211. <https://doi.org/10.1007/s00445-012-0594-0>
- Hasenaka T (1994) Size, distribution and magma output rates for shield volcanoes of the Michoacán-Guanajuato volcanic field, Central Mexico. *J Volcanol Geotherm Res* 63(1-2):13–31. [https://doi.org/10.1016/0377-0273\(94\)90016-7](https://doi.org/10.1016/0377-0273(94)90016-7)
- Hasenaka T, Carmichael ISE (1985a) A compilation of location, size, and geomorphological parameters of volcanoes of the Michoacán-Guanajuato volcanic field, central Mexico. *Geofis Int* 24(4):577–607
- Hasenaka T, Carmichael ISE (1985b) The cinder cones of Michoacán-Guanajuato, central Mexico: their age, volume and distribution, and magma discharge rate. *J Volcanol Geotherm Res* 25(1-2):105–124. [https://doi.org/10.1016/0377-0273\(85\)90007-1](https://doi.org/10.1016/0377-0273(85)90007-1)
- Hasenaka T, Carmichael ISE (1987) The cinder cones of Michoacán-Guanajuato, central Mexico: petrology and chemistry. *J Petrol* 28(2):241–269. <https://doi.org/10.1093/petrology/28.2.241>
- INEGI (2016) Instituto Nacional de Estadística, Geografía e Informática, National Census website: <http://cuentame.inegi.org.mx/monografias/informacion/Mich/Poblacion/default.aspx?tema=ME&e=16>
- Johnson CA, Harrison CGA (1990) Neotectonics in Central Mexico. *Phys Earth Planet Inter* 64(2-4):187–210. [https://doi.org/10.1016/0031-9201\(90\)90037-X](https://doi.org/10.1016/0031-9201(90)90037-X)
- Johnson ER, Wallace PJ, Granados HD, Manea VC, Kent AJ, Bindeman IN, Donegan CS (2009) Subduction-related volatile recycling and magma generation beneath Central Mexico: insights from melt inclusions, oxygen isotopes and geodynamic models. *J Petrol* 50(9):1729–1764. <https://doi.org/10.1093/petrology/egp05>
- Kim Y, Miller MS, Pearce F, Clayton RW (2012) Seismic imaging of the Cocos plate subduction zone system in central Mexico. *Geochem Geophys Geosyst* 13(7):Q07001. <https://doi.org/10.1029/2012GC004033>
- Kshirsagar P, Siebe C, Guilbaud M-N, Salinas S, Layer PW (2015) Late Pleistocene Alberca de Guadalupe maar volcano (Zacapu basin, Michoacán): stratigraphy, tectonic setting, and paleo-hydrogeological environment. *J Volcanol Geotherm Res* 304:214–236. <https://doi.org/10.1016/j.jvolgeores.2015.09.003>
- Kshirsagar P, Siebe C, Guilbaud MN, Salinas S (2016) Geological and environmental controls on the change of eruptive style (phreatomagmatic to Strombolian-effusive) of Late Pleistocene El Caracol tuff cone and its comparison with adjacent volcanoes around the Zacapu basin (Michoacán, México). *J Volcanol Geotherm Res* 318:114–133. <https://doi.org/10.1016/j.jvolgeores.2016.03.015>
- Layer PW (2000) $^{40}\text{Ar}/^{39}\text{Ar}$ age of the El'gyygtin impact event, Chukotka, Russia. *Meteorit Planet Sci* 35(3):591–599. <https://doi.org/10.1111/j.1945-5100.2000.tb01439.x>
- Le Maitre RW (2002) Igneous rocks: a classification and glossary of terms: recommendations of the International Union of Geological Sciences Subcommittee on the systematics of igneous rocks. Cambridge University Press, 273 pp, Cambridge. <https://doi.org/10.1017/CBO9780511535581>
- Lozano-García MS, Xelhuantzi-López MS (1997) Some problems in the Late Quaternary pollen records of central Mexico: basins of Mexico and Zacapu. *Quat Int* 43/44:117–123. [https://doi.org/10.1016/S1040-6182\(97\)00027-X](https://doi.org/10.1016/S1040-6182(97)00027-X)
- Luhr JF, Simkin T (1993) Paricutin: the volcano born in a Mexican cornfield. Geoscience Press, 427 pp
- Mahgoub AN, Böhnell H, Siebe C, Chevrel MO (2017a) Paleomagnetic study of El Metate shield volcano (Michoacán, Mexico) confirms its monogenetic nature and young age (~1250 CE). *J Volcanol Geotherm Res* 336:209–218. <https://doi.org/10.1016/j.jvolgeores.2017.02.024>
- Mahgoub AN, Reyes-Guzmán N, Böhnell H, Siebe C, Pereira G, Dorison A (2017b) Paleomagnetic constraints on the ages of the Holocene Malpaís de Zacapu lava flow eruptions, Michoacán (Mexico): implications for archeology and volcanic hazards. The Holocene: 095968361772132. <https://doi.org/10.1177/0959683617721323>
- Mahgoub AN, Böhnell H, Siebe C, Salinas S, Guilbaud M-N (2017c) Paleomagnetically inferred ages of a cluster of Holocene monogenetic eruptions in the Tacámbaro-Puruarán area (Michoacán, México): implications for volcanic hazards. *J Volcanol Geotherm Res* 347:360–370. <https://doi.org/10.1016/j.jvolgeores.2017.10.004>
- Metcalfe SE (1997) Paleolimnological record of the climate change in México-frustrating past, promising future? *Quat Int* 43:111–116
- Michelet D (1992) El Centro-Norte de Michoacán: características generales de su estudio regional. In: Darras V (ed) Génesis, culturas y espacios en Michoacán. CEMCA, México, pp 9–52
- Michelet D (1998) Topografía y prospección sistemática de los grandes asentamientos del Malpaís de Zacapu: claves para un acercamiento a las realidades sociopolíticas. In: Darras V (ed) Génesis, culturas y espacios en Michoacán. CEMCA, México, pp 47–59. <https://doi.org/10.4000/books.cemca.3396>
- Michelet D (2010) De palabras y piedras: reflexiones en torno a las relaciones entre arqueología e historia en el Michoacán prehispánico, sector Zacapu. *Istor* 11(43):27–43
- Michelet D, Arnauld MC, Fauvet-Berthelot MF (1989) El proyecto del CEMCA en Michoacán. Etapa I: un balance TRACE 16:70–87
- Michelet D, Pereira G, Migeon G (2005) La llegada de los uacúsechas a la región de Zacapu, Michoacán; Datos arqueológicos y discusión. In: Manzanilla L (ed) Reacomodos demográficos del Clásico al Posclásico en el centro de México. Instituto de Investigaciones Antropológicas, UNAM, México, pp 137–153
- Migeon G (1998) El poblamiento del Malpaís de Zacapu y de sus alrededores del Clásico al Posclásico. In: Darras V (ed) Génesis, culturas y espacios en Michoacán. CEMCA, México, pp 36–45. <https://doi.org/10.4000/books.cemca.3395>
- Noriega E, Noriega A (1923) La desecación de la ciénega de Zacapu y las leyes agrarias. Caso especial, único en el país. México
- O'Hara SJ, Street-Perrott FA, Burt TP (1993) Accelerated soil erosion around a Mexican highland lake caused by pre-Hispanic agriculture. *Nature* 362(6415):48–51. <https://doi.org/10.1038/362048a0>
- Ortega-Guerrero B, Caballero M, Lozano-García S, Israde I, Vilaclara G (2002) 52,000 years of environmental history in Zacapu basin, Michoacán, México: the magnetic record. *Earth Planet Sci Lett* 202:663–675
- Ownby SE, Delgado-Granados H, Lange RA, Hall CM (2007) Volcán Tancitaro, Michoacán, México. $^{40}\text{Ar}/^{39}\text{Ar}$ constraints on its history of sector collapse. *J Volcanol Geotherm Res* 161(1-2):1–14. <https://doi.org/10.1016/j.jvolgeores.2006.10.009>
- Pardo M, Suárez G (1995) Shape of the subducted Rivera and Cocos plates in southern Mexico: seismic and tectonic implications. *J Geophys Res* 100(B7):12357–12373. <https://doi.org/10.1029/95JB00919>
- Pereira G, Forest M, Jadot E et al (2017, in press) Ephemeral cities? The longevity of the Postclassic Tarascan urban sites of Zacapu Malpaís and its consequences on the migration process. In: Arnauld M-C, Beekman C, Pereira G (eds) Ancient Mesoamerican Cities: Populations on the Move. University Press of Colorado, Boulder

- Pétrequin P (1994) 8000 años de la cuenca de Zacapu. *Centre de Etudes Mexicaines et Centroamericaines, Mexico. Cuadernos de Estudios Michoacanos* 6, 144 pp
- Piña-Chan R (1972) Teotenango Primer informe de exploraciones arqueológicas, enero a septiembre de 1971. Dirección de Turismo, Gobierno del Estado de México, Toluca 34 pp
- Pioli L, Erlund E, Johnson E, Cashman KV, Wallace P, Rosi M, Delgado H (2008) Explosive dynamics of violent Strombolian eruptions: the eruption of Parícutin volcano 1943-1952 (Mexico). *Earth Planet Sci Lett* 271(1-4):359-368. <https://doi.org/10.1016/j.epsl.2008.04.026>
- Pola A, Macías JL, Garduño-Monroy VH, Osorio-Ocampo S, Cardona-Melchor S (2014) Successive collapses of the el Estribo volcanic complex in the Pátzcuaro Lake, Michoacán, Mexico. *J Volcanol Geotherm Res* 289:41-50. <https://doi.org/10.1016/j.jvolgeores.2014.10.011>
- Pollard HP (1993) Tariácuri's legacy. The Prehispanic Tarascan State. University of Oklahoma Press, Norman 256 pp
- Pollard HP (2003) Central places and cities in the core of the Tarascan stae. In: Sanders WT, Mastache AG, Cobean RH (eds) *Urbanism in Mesoamerica Vol. 1*, Instituto Nacional de Antropología e Historia and Pennsylvania State University, pp 345-390
- Pollard HP, Cahue L (1999) Mortuary patterns of regional elites in the lake Pátzcuaro basin of western Mexico. *Lat Am Antiq* 10(3):259-280. <https://doi.org/10.2307/972030>
- Rasoazanamparany C, Widom E, Siebe C, Guilbaud M-N, Spicuzza MJ, Valley JW, Valdez G, Salinas S (2016) Temporal and compositional evolution of Jorullo volcano, Mexico: implications for magmatic processes associated with a monogenetic eruption. *Chem Geol* 434:62-80. <https://doi.org/10.1016/j.chemgeo.2016.04.004>
- Renne PR, Mundil R, Balco G, Min K, Ludwig KR (2010) Joint determination of 40K decay constants and 40Ar*/40K for the Fish Canyon sanidine standard, and improved accuracy for ⁴⁰Ar/³⁹Ar geochronology. *Geochimica Cosmochim Acta* 74(18):5349-5367. <https://doi.org/10.1016/j.gca.2010.06.017>
- Reyes-Guzmán N (2017) Geología volcánica de la región occidental de la cuenca lacustre de Zacapu, Michoacán y su importancia para la arqueología. Facultad de Ciencias, Universidad Nacional Autónoma de México, México 113 pp
- Siebe C, Guilbaud M-N, Salinas S, Chedeville-Monzo C (2012) Eruption of Alberca de los Espinos tuff cone causes transgression of Zacapu lake ca. 25,000 yr BP in Michoacán, Mexico. In: Arentsen K, Nemeth K, Smid E (eds) *Abstract Volume of the Fourth International Maar Conference. A Multidisciplinary Congress on Monogenetic Volcanism*, Auckland, New Zealand (20-24 February 2012). *Geoscience Society of New Zealand Miscellaneous Publication 131A*: 74-75 (ISSN Online 2230-4495)
- Siebe C, Guilbaud M-N, Salinas S, Layer P (2013) Comparison of the volcanic geology of the Tacámbaro-Puruarán (arc front) and the Zacapu (arc inland) areas in the Michoacán-Guanajuato volcanic field, México. IAVCEI 2013 Scientific Assembly, July 20-24. Kagoshima, Japan. Abstract volume
- Siebe C, Guilbaud M-N, Salinas S, Kshirsagar P, Chevrel MO, De la Fuente, JR, Hernández-Jiménez, A, Godínez L (2014) Monogenetic volcanism of the Michoacán-Guanajuato volcanic field: Maar craters of the Zacapu basin and domes, shields, and scoria cones of the Tarascan highland (Paracho-Parícutin region). In: *Field guide, Pre-meeting Fieldtrip for the 5th International Maar Conference (SIMC-IAVCEI)*. Querétaro, 13-17 November, 33 pp
- Stuiver M, Reimer PJ (1993) Extended ¹⁴C database and revised CALIB radiocarbon calibration program. *Radiocarbon* 35(01):215-230. <https://doi.org/10.1017/S0033822200013904>
- Suter M, López-Martínez M, Quintero-Legorreta O, Carrillo-Martínez M (2001) Quaternary intra-arc extension in the central Trans-Mexican volcanic belt. *Bull Geol Soc Am* 113(6):693-703. [https://doi.org/10.1130/0016-7606\(2001\)113<0693:QIAEIT>2.0.CO;2](https://doi.org/10.1130/0016-7606(2001)113<0693:QIAEIT>2.0.CO;2)
- Torres-Rodríguez E, Lozano-García S, Figueroa-Rangel BL, Ortega-Guerrero B, Vázquez-Castro G (2012) Cambio ambiental y respuestas de la vegetación de los últimos 17,000 años en el centro de México: el registro del lago de Zirahuén. *Rev Mex Cienc Geol* 29(3):764-778
- Watts WA, Bradbury JP (1982) Paleocological studies at Lake Patzcuaro on the west-central Mexican Plateau and at Chalco in the Basin of Mexico. *Quat Res* 17(01):56-70. [https://doi.org/10.1016/0033-5894\(82\)90045-X](https://doi.org/10.1016/0033-5894(82)90045-X)